HELSINGIN YLIOPISTO
HELSINGFORS UNIVERSITET
UNIVERSITY OF HELSINKI
LÄÄKETIETEELLINEN TIEDEKUNTA
MEDICINSKA FAKULTETEN
FACULTY OF MEDICINE

The generation of a T reporter cell line based screening method for T-cell receptor functional testing

Fanny Erkkilä

Bachelor of Medicine

Hematology Research Unit Helsinki, University of Helsinki and Helsinki University Hospital Comprehensive Cancer Center

Translational Immunology Research Program and Department of Clinical Chemistry and Hematology, University of Helsinki.

Helsinki 11.11.2022

Advanced studies thesis

fanny.erkkila@helsinki.fi

Supervisor: Ph.D. Karita Peltonen, Prof. Satu Mustjoki

Faculty of Medicine

UNIVERSITY OF HELSINKI

Abstract

Faculty: Faculty of Medicine

Programme: Degree Programme in Medicine

Study orientation: Swedish orientation

Author: Fanny Erkkilä

Title: The generation of a T reporter cell line based screening method for T-cell receptor functional testing

Level: Advanced studies thesis

Month and year: November 2022

Pages: 61

Keywords: Immunotherapy, t-cell receptor, t-lymphocytes, co-culture screen

Where deposited: Student saves electronic version to E-thesis

Additional information:

Abstract: The immune system recognizes foreign entities in the body and induces protective responses. Sometimes, the immune system does not work optimally, which can lead to different clinical manifestations, one of which is cancer. T cells are a part of the immune system and has the ability to recognize and eliminate the body's own cells that have transformed into cancer cells. In the field of immuno-oncology, a vast body of research is focusing on understanding the relationship between cancer and the immune system, as well as developing strategies to eliminate cancer by utilizing the immune system. The rise of computational approaches, that can analyze large amounts of data from single-cell sequencing techniques, have enabled the field to conduct research on a new level of complexity. However, this powerful tool has not yet reached its full potential, one major challenge is the lack of functional data of T-cell receptor recognition. In this thesis, we are focusing on the T-cell receptor mediated therapies against cancer, and work toward setting up a screen that assesses T-cell receptor specificity and functionality, which is a powerful tool to acquire knowledge of T-cell biology and improve immunotherapies. One can postulate that

the functional data produced by functional screens could be used to train prediction algorithms to a degree, where we could predict the specificity of a TCR based on raw sequencing data.

(225 words)

Sammanfattning: Immunsystemet känner igen kroppsfrämmande komponenter och aktiverar skyddsmekanismer för att eliminera inkräktaren. Ibland fungerar inte immunsystemet optimalt, vilket kan leda till olika kliniska manifestationer, var av en är cancer. T-lymfocyter är en del av immunsystemet och har en förmåga att känna igen och eliminera kroppsegna celler som har förändrats till cancerceller. Inom den heta forskningsområdet immunonkologi, arbetar forskare mot att förstå relationen mellan cancerceller och immunsystemet, samt utvecklar immunoterapier som strävar till att eliminera cancer genom att använda sig av immunsystemets komponenter. Framsteg i bioinformatik har möjliggjort hantering och analys av stora mängder data från sekvensering av enskilda celler, och därmed tagit forskningen till en ny nivå av komplexitet. Metoden har dock inte än nått sin fulla potential, en utmaning är bristen av funktionell data av T-cellreceptorn. I denna avhandling, fokuserar vi på T-cell-medierade immunoterapier och arbetar mot att bygga upp en screeningmetod för att undersöka T-cellreceptorns igenkänningsförmåga och funktion. Denna kraftiga metod kan användas för att få baskunskap om T-cellens biologi och utveckla immunoterapier. Man kan även postulera, att med hjälp av den funktionella data som screeningmetoden ger, är det möjligt att träna algoritmer till den grad, att vi kan förutsäga en viss T-cellreceptors specificitet bara på basis av den sekvenserade receptorns rådata.

(204 ord)

Table of contents

1 Introduction

The immune system recognizes foreign entities in the body and induces protective responses. To fulfill this task, the immune system needs to recognize the foreign pathogen, eliminate it and self-regulate to avoid damage to the body itself. Furthermore, the immune system is capable of generating immunological memory, which means that if the immune system encounters the same foreign invader again, it can mobilize fast and effectively against it.

T lymphocytes (T cells) are a part of the immune system that have the ability to recognize and eliminate the body's own cells that have become infected by a pathogen or that have transformed into cancer cells. Sometimes, the immune system does not work optimally, and the T cells cannot eliminate the cancer cells, which can lead to the different clinical manifestations of cancer. A vast body of research has emerged under the topic of immuno-oncology, where the aim is to understand the functional relationship between cancer cells and the immune system, and to develop therapies that utilizes the immune system to eliminate cancer.

The thesis consists of two parts: a literature overview and an experimental part. The literature overview presents the biological background of the T-cell receptor (TCR) function, how different immunotherapies against cancer utilizes TCRs, and different methods that assess the specificity of TCRs used to increase the understanding of TCR biology and to improve immunotherapies. By presenting the biology of T-cells and its current applications in immunotherapy, the literature overview also gives context to the experimental part of the thesis, which describes the work we did toward setting up a cell-based co-culture screen that assesses TCR-specificity and functionality.

The aim of the literature review is to give the adequate biological background to understand TCR function, present how TCRs can be utilized in immunotherapies, and describe different ways to assess TCR specificity.

2 Literature review

2.1 The biology of T cells

The immune system is divided into the innate and adaptive immune system. The innate immune system is the body's first line of defense that eliminates non-specifically all pathogens that tries to invade the body. If the pathogens overwhelm or evade the innate immune system, the adaptive immune system steps in to help. The effectiveness of the adaptive immune system lies in its ability to detect the specific pathogen and manufacture a tailored attack against it. The adaptive immune system encounters a new pathogen via antigen-presenting cells (APCs), that patrol in the body and ingests various microscopic matter that it encounters. After ingestion, the cell metabolizes the ingested material and produces a short peptide that represents the character of the material. This peptide is called an antigen and it expresses whether the metabolized material is endogenous or not. When a lymphocyte encounters an APC that presents an antigen that is not endogenous, the lymphocyte will be activated and start a cascade of events that result in the elimination of all cells that present this specific antigen. These cells can be the pathogen itself or endogenous cells that the pathogen has infected. The elimination mechanisms used in these different scenarios are different, in this text we will focus on T cells that mediate the elimination of cells that express non-self antigens. When the pathogen is eliminated, all effector cells undergo apoptosis except for a little group of cells that will establish the memory cell populations. Next time the adaptive immune system encounters the same pathogen, memory cells are activated and eliminates the pathogen rapidly (1).

T cells develop from pluripotent hematopoietic stem cells in the bone marrow and become common lymphoid progenitor cells, which in turn mature in the thymus to naïve T cells. In the thymus the cells undergo a selection that eliminates all candidates that do not recognize self antigens at all or recognize self antigens in such an extent that would lead to autoreactivity. The cells also get their identity, cytotoxic T cells eliminate target cells, whereas T helper cells regulate the elimination process (2).

2.1.1 T-cell antigen recognition and T-cell activation

The cytotoxic T cell's elimination process starts with the recognition of an antigen with its antigen receptor, TCR. Each T cell has one TCR with unique antigen recognition sites, and together the billions of lymphocytes in the body hold a vast antigen receptor repertoire with which the lymphocytes can recognize virtually any pathogen the body encounters. But TCRs cannot recognize an antigen in its free form, instead the antigen needs to be presented on a major histocompatibility complex (MHC) molecule. MHC molecules comes in two classes, MHC class I and MHC class II, and they interact with CD8 positive T cells ($CD8^+$ T cells) and CD4 positive T helper cells ($CD4^+$ T cells), respectively (3). These cell types are effective at eliminating different kind of pathogens and the MHC molecules help directing the cells against the pathogens which they are specialized to eliminate.

MHC class I molecules are expressed by all cells except red blood cells. MHC class I molecules are synthetized in the endoplasmic reticulum, where a part of a cytosolic protein is added to the MHC molecule which results in a peptide:MHC complex (pMHC), that will be presented on the cell surface. If a cell is infected by a virus or bacteria that replicates in the host cell's cytoplasm, a part of the virus or bacteria, an antigen, is presented on the MHC class I molecule. Now, a cytotoxic T cell can bind to the invariant part of the MHC class I molecule with its co-receptor CD8 and recognize the non-self antigen with the TCR, forming a TCR:pMHC interaction, and proceed to eliminate the infected cell (4).

MHC class II molecules are expressed by macrophages, dendritic cells, B cells and T cells. Additionally, thymic cortical epithelial cells, that take part in the T cell training in the thymus, express MHC class II molecules. The MHC class II molecules present peptides from proteins that are degraded in endosomes. Endosomes are formed when cells endocytose extracellular material, for example when macrophages ingest bacteria or parasites. Some pathogens do not degrade in the vesicle system of macrophages and start replicating instead. When MHC class II molecules present an antigen of the pathogen on the host-cell's surface, T helper cells can bind to the MHC class II molecule with the co-receptor CD4 and become activated. There are many subsets of $CD4^+$ T cells with different effects, for example an activated T helper cell can boost the infected macrophage so that it will be able to eliminate the pathogen itself.

$CD4^+$ T cells can also be cytotoxic and there is significant crosstalk between the pathways of $CD4^+$ and $CD8^+$ T cells (5).

T cells are able to recognize antigens with their TCRs and co-receptors but to initiate an activation cascade the T cell need additional signals from co-stimulatory receptors. The best understood co-stimulatory receptor is CD28, which is expressed on the surface of all naïve T cells. CD28 binds to B7-family ligands that are B7.1 (CD80) and B7.2 (CD86) (Figure 1). These molecules are expressed mainly on APCs during an infection (6). This ensures that a T cell is not activated if it recognizes an antigen on a non-infected cell. When CD28 binds to a B7-family ligand, the DAG-IP_3 cascade is initiated that in turn activates the transcription factors nuclear factor of activated T cells (NFAT), transcription factor AP-1 (AP-1) and transcription factor NF-κB (NF-κB). These transcription factors stimulate the expression of IL-2 genes, which plays a key role in T cell proliferation and differentiation (7).

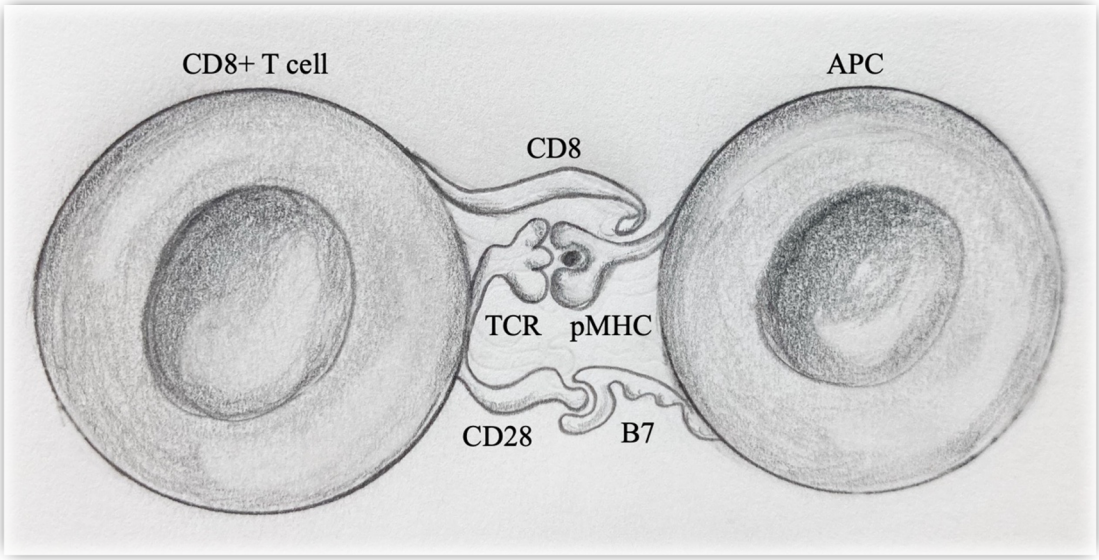

Figure 1. Signal 1, signal 2 and signal 3 that lead to T-cell activation. To achieve T-cell activation, the $CD8^+$ T cell needs three signals from the APC. Firstly, in signal 1 the TCR recognizes a peptide bound to an MHC class I molecule. Secondly, in signal 2 the co-receptor CD8 binds to the invariant part of the MHC class I molecule. Thirdly, in signal 3 the co-stimulatory receptor CD28 binds to the B7-family proteins.

At the same time as CD28 binds to its ligand and starts the activation cascade, the expression of the inhibitory receptor cytotoxic lymphocyte antigen-4 (CTLA-4) is stimulated. CTLA-4 normally resides inside the cell but when TCR signaling is activated it moves to the cell surface and competes with CD28 of binding to the same B7-family ligands. When CTLA-4 binds to the B7-ligans it results in an inhibitory effect on the T cell activation and regulates the immune response. It is not clear how the inhibitory effect is accomplished, but it may be a result from inhibiting the binding of CD28 to its ligands and therefore inhibiting the co-stimulatory signaling from CD28. Another important inhibitory receptor is programmed death-1 (PD-1). When PD-1 is activated it starts a signaling cascade that results in the dephosphorylation of PIP_3 and thus reverses the recruitment of proteins needed for T-cell activation. PD-1 can bind to the B7-family ligands programmed death ligand-1 (PD-L1) and programmed death ligand-2 (PD-L2). PD-L1 is expressed on a wide variety of cells constitutively and its expression is repressed by pro-inflammatory cytokines (8).

The activation cascade results in the synthesis of IL-2 proteins and receptors, and the T cell will start proliferating 2-3 times a day resulting in thousands of daughter cells (9). Next, the daughter cells will differentiate into effector cells that are capable of eliminating target cells. The cytotoxic T cell scans potential target cells surface by binding to it with non-antigen specific interactions. If the scanned cell does not have the target antigen, the cytotoxic T cell disengages and moves on to the next potential target cell. When the cytotoxic T cell finds a cell with the target antigen, it forms a TCR:pMHC interaction, which stimulates the cytotoxic T cell to release preloaded cytotoxic granules onto the target cell. The cytotoxins are non-specific, which indicates that the toxins diffuse across cell membranes and induces apoptosis in all cells. The binding of TCR also stimulates the production of more cytotoxic granules and thereby allows one cytotoxic T cell to eliminate many target cells in succession. Lastly, the TCR binding also stimulates the release of cytokines in the close microenvironment that will increase the expression of MHC class I molecules on cells nearby, and therefore increases the T cell's chances to find a new target cell (10).

2.1.2 The T-cell receptor

When we take a closer look at the TCR, we see that the TCR consists of two different chains that are linked by a disulfide bond: T cell receptor α (TCRα) and T cell receptor β (TCRβ).

The majority of T cells bear α:β heterodimers (TCRαβ), and a minority of T cells bear γ:δ heterodimers that consists of a different pair of polypeptide chains (11). In the rest of this thesis the term TCR indicates the α:β receptor.

Both chains of the TCR have a variable (V) region, a constant (C) region and a stalk segment that forms the disulfide bond. The chains have a hydrophobic transmembrane domain and a short cytoplasmic tail. The most important part for T cell recognition is the third hypervariable region (CDR3) that makes a loop from the V-region and is the site that lies over the central part of the peptide. When the TCR is bound to a pMHC, the TCRα chain is placed over the α_2 domain and the amino-terminal end of the bound peptide, and the TCRβ chain is placed over the α_1 domain and the carboxy-terminal end of the peptide. Both TCRα and TCRβ chain CDR3 loops are placed over the central amino acids of the bound peptide (12) (Figure 2).

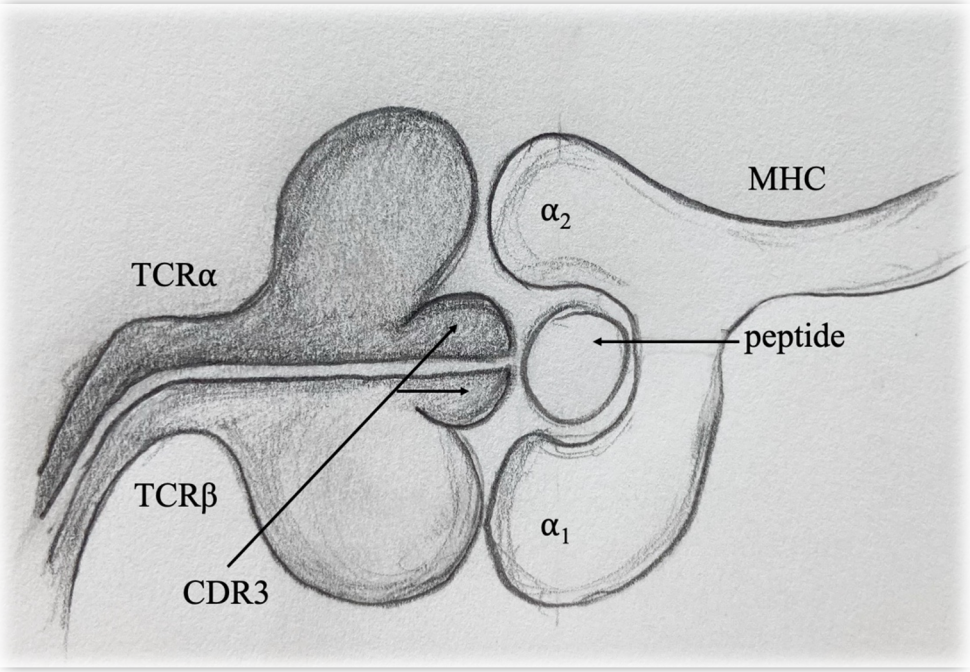

Figure 2. TCR:pMHC interaction. The TCR consists of two chains: TCRα and TCRβ. When the TCR binds to a pMHC, the TCRα binds to the α_2 domain of the MHC molecule, and the TCRβ binds to the α_1 domain. Both chains contain a hypervariable region called CDR3, that binds to the central amino acids of the peptide.

The wide repertoire of antigens that TCRs can recognize is due to the variation in the antigen-binding site's amino acid sequence, in the V-region's CDR3 sequence. Every TCR-chain's V-region cannot have an own gene because the number of genes would exceed the genes in the genome. Instead, there are two processes creating diversity in the antigen recognition site: combinatorial diversity and junctional diversity (1). The combinatorial diversity starts in the chromosomes. The gene coding for the V-region is chopped up to two or three segments and the segments are multiplied in the germline genome. Then, by a mechanism called gene rearrangement, random combinations of these gene segments are assembled to a complete V-region by somatic DNA recombination. The junctional diversity is created by random additions and deletions of nucleotides between all V and J gene segments of rearranged TCRα genes, which is also the location of CDR3 (11).

These mechanisms have the potential to generate a large diversity of TCRs. There are two types of T cell repertoires. Firstly, there is the vast TCR repertoire that consists of all possible sequences of TCRα and TCRβ, and their potential pairings that are estimated (11,13) to range from 10^{15} to 10^{61}. Secondly, there is the ligand repertoire which is approximately one thousand times smaller (10^{12}), a much more manageable figure for most purposes, and is often biologically more relevant (14).

2.1.3 Why does not the immune system eliminate cancer cells?

Cancer cells arise from healthy somatic cells as a result from DNA mutations that reprogram the cell from serving the organ system to directing all its efforts to survive and expand. In order to thrive, the cancer cell needs to evade the attacks directed on it by the immune system. As a consequence of the cancer cells' high mutation frequency, deficiencies in their DNA repair system and that the cells are under selection pressure, phenotypes of cancer cells with immunosuppressive mechanisms can arise (15) (Figure 3).

The immunosuppressive mechanisms are not fully understood, but we can paint a picture of the subject by looking at some tumors' responses to immunotherapies. Some cancer cells have the ability to express molecules that inhibit immune cell activity, such as PD-L1 that is the ligand for PD-1 on immune cells. Immune checkpoint inhibitors (ICIs) are antibodies targeting these inhibiting molecules. By administering ICIs, the immunological "breaks" are

lifted, and the immune system can eliminate cancer cells. One could postulate, that in these tumors there is a pre-existing antitumor immunity that can be rejuvenated with ICIs (16). These therapies have had impressive results on some cancers, for example among patients with advanced melanoma, where some are still alive ten years after ICIs treatment (17). However, most cancer patients do not respond to ICIs and therefore cancer cells' expression of inhibitory molecules is not the only way around the immune system (18).

For a successful immune response against cancer cells, it is vital that the immune cells recognize the cancer cell. Neoantigens are new antigens that leukocytes recognize as foreign, these can emerge from spontaneous mutations. Cancers can be classified by their genotype into high and low tumor mutational burdens, where the high tumor mutational burden has often a higher expression of neoantigens and a better response to ICIs. Some cancer cells can down-regulate their expression of MHC-molecules, resulting in no antigen presentation even if the cells have neoantigens. An interesting observation is that some virally-induced cancers have better responses to ICIs than their non-virally-induced counterparts, suggesting that viral neoantigens help the immune system to recognize the cancer cell (16).

A high mutation rate is not necessarily equal to a high level of immune infiltration. Cancer cells have the ability to generate physical barriers that stop T-cells from infiltrating the tumor. In their paper, Mariathasan et al. (19), identified determinants of clinical outcomes of ICIs treated patients with metastatic urothelial cancer, and found that a lack of response was associated with transforming growth factor β (TGFβ) signaling in fibroblasts. This occurred especially in patients where $CD8^+$ T cells were excluded from the tumor parenchyma and stuck in the peritumoral stroma rich in fibroblasts and collagen. When they co-administered the ICI and TGFβ-blocking antigens in a mouse-model, the T-cells were able to penetrate into the tumor center and eliminate the tumor.

Lastly, yet to be identified immunosuppressive mechanisms can turn tumor-reactive cytotoxic T cells into an exhausted sate. Normally when naïve T cells recognize an antigen, the TCR-mediated signaling pathways stimulate the cells to proliferate and differentiate to active cytotoxic T cells and resting memory cells. However, if the antigen presentation is prolonged, for example during a chronic infection or in cancer, the differentiation to memory cells is inhibited and the T cell will be stimulated to proliferate time and time again, which will lead to multiple cell population doublings. This type of activity shifts T cells to a

senescent state, which is an irreversible non-functional state that ends in activation-induced cell death by apoptosis (20). Before T cells reach this point, it is possible to turn them into an exhausted state. This can happen if the chronic antigen presentation is paired with specific extrinsic factors, such as a heightened inflammatory status and the absence of $CD4^+$ T cells. Exhausted T cells are physiologically intact but have reduced functionality, and the exhausted state can be reversed. Reactivation of these cells could have a profound anti-tumor effect (21).

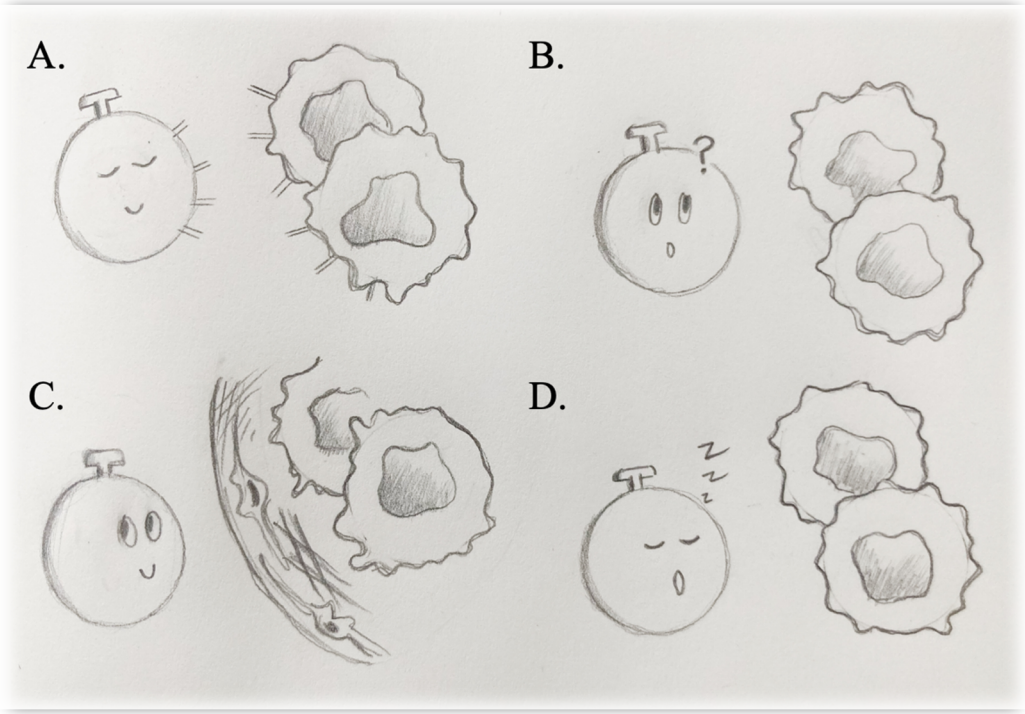

Figure 3. Different immunosuppressive mechanisms. (A) Cancer cells can express proteins that inhibit T-cell activation such as CTLA-4 and PD-1. (B) Some cancer cells have a low rate of neoantigens, which can inhibit T cells from recognizing them. Cancer cells can also down-regulate their MHC-expression, which results in no antigen presentation even if the cancer cell has neoantigens. (C) Some forms of cancer can build a physical barrier by activating fibroblasts that produce collagen, which results in that T cells cannot infiltrate the tumor. (D) Some yet to be defined mechanisms can cause T cells to go into an inactivated state called senescence.

2.2 Immunotherapies

Adoptive T cell transfer is a promising approach of cancer treatment, where the patient's T cells are isolated from the patient and genetically modified to become more tumor-reactive, and then transfused back into the patient's body to eliminate the target cells. There are four adoptive T cell transfer techniques developed: chimeric antigen receptor T-cell therapy (CAR-T), T-cell receptor engineered T-cell therapy (TCR-T), tumor-infiltrating lymphocyte (TIL) therapy, and antigen-specific endogenous T-cell therapy (ETC). In CAR-T and TCR-T therapies, T cells are genetically modified to express receptor with high affinity to target antigens. In TIL therapy and ETC, T cells are isolated from the patient's tumor or peripheral blood, respectively, and expanded in vitro to finally infuse them back to patients (22). Therapeutic cancer vaccines will also be discussed.

The largest number of therapeutic agents in immuno-oncology are cell therapies. As of April 2021, there were 2,073 active cell therapy agents in the global cell therapy pipeline, with a 38% increase from 2020. Of the different types of cell therapies, CAR-T cells is the largest group with 1,164 agents in the pipeline and a 35% increase from 2020 (23). Other cell therapy classes with increased number of new agents are TCR T cell therapy (80 new agents), NK/NKT cells (67 new agents), novel T cells (51 new agents), and TILs (33 new agents).

2.2.1 CAR-T therapy

In CAR-T cell therapy, T cells are isolated from blood and modified to express a chimeric antigen receptor (CAR), which enables the T cell to recognize and eliminate cancer cells without having to bind to a pMHC complex. MHC-independent antigen recognition is advantageous if the cancer cell has downregulated or mutated MHC molecules (24). The CARs have evolved from consisting of an extracellular binding domain, a transmembrane domain, and an intracellular domain coupled to proteins driving T-cell proliferation and cytokine secretion, to including costimulatory molecules and the secretion of cytokines (24). CAR-T cell therapy efficacy for treating acute B lymphocytic leukemia has been widely recognized, all five anticancer cell therapies approved by FDA are CAR-T cell therapies, four have CD19 as a target and the most recently approved therapy targets B cell maturation

antigen (BCMA) (23). CD19 and BCMA are B-cell specific molecules, and consequently, the CAR-T cells deplete not only the cancer cells, but also healthy $CD19^+$ B cells during treatment. However, B cells are temporarily expendable, and the normal B cell population can be restored after the treatment, and thus the depletion of B cells is regarded as an acceptable toxicity.

The limitations of CAR-T cell therapy that casts a shadow on the development are poor CAR-T expansion, tumor cells with deletion or mutation of the target molecule, potential lethal toxicities, high-cost and labor-intensive production that takes 2 weeks, during which aggressive cancer types can continue to progress, other cancer therapies can cause lymphocytopenia resulting in inadequate T cells for CAR-T cell production. Currently universal CAR-T (UCAR-T) cell therapy is under development in hope to upgrade the approach. The existing CAR-T therapies in development and on the market are made with T-cells from the patient that will receive the therapy to ensure matching MHCs and therefore avoid alloimmune rejection, whereas in UCAR-T therapy the T cells would be isolated from healthy donors. This approach could evolve the customized CAR-T therapy into a universal therapy by enabling large-scale production and therefore increase accessibility. Initial successful attempts have been made, but challenges such as alloimmune rejection and the short-persistence of UCAR-T cells, needs to be solved before the approach enters the clinic (25).

2.2.2. TCR-T therapy

In TCR-T cell therapy, an artificial TCR with high affinity to the cancer antigen is expressed in the patient's T cells. This artificial TCR contains all auxiliary molecules needed for T-cell activation and it requires the antigen to be presented on an MHC molecule. This allows the artificial TCR to recognize both antigens on the cell surface and intracellular antigens presented on MHC molecules.

The optimal target for TCR-T therapy has the ability to elicit an immune response, it is associated with tumor-driving phenotypes, and the target is expressed on cancer stem cells to drive long-lasting tumor eradication (26). Initially, TCR-T cells were targeting shared

tumor-associated antigens (TAAs), that are peptides originating from endogenous wild-type proteins expressed in a higher magnitude on tumor cells but less in healthy tissues. The New York esophageal squamous cell carcinoma 1 (NY-ESO-1), which is expressed in many cancers including melanoma and myeloma, is the most popular TAA target in TCR-T clinical trials, and it has achieved an objective response rate of 67% in treating synovial sarcoma (27). The majority of acute leukemias express the Wilms tumor gene product 1 (WT1) and using TCR-T cells targeted against WT1 has shown great promise as the T cells eliminate the cancer cells but do not inhibit human hematopoiesis (28). In virus-associated cancer types, TCR-T therapy can target viral antigens. In a Phase 1 clinical trial, TCR-T cells were modified to target human papillomavirus (HPV) 16 E7 protein for treating HPV-associated epithelial cancers, and the treatment showed an objective clinical response with tumor regression in 6 of 12 treated patients (29). Upon recent technological advancements, TCR-T cells have been engineered to target neoantigens, that are antigens acquired from tumor somatic mutations. Neoantigens are highly specific to cancer cells and appear to be the safest targets in the context of immune toxicities. Then again, the mutations giving rise to neoantigens are highly heterogenous across tumor tissues and differ between cancer patients, which makes it difficult to find widely applicable targets (22).

As of April 2021, there were 214 TCR-T cell therapy agents in the global pipeline and a 60% increase from 2020 (23). Clinical TCR-T Phase 1 trials' overall response rates range from 0%-60%, and almost 50 % of the trials has not reported the clinical response rates. The lack of continuous clinical success can stem of some of the following challenges faced in TCR-T therapy: toxicity caused by targeting healthy tissues, inadequate TCR expression in modified T cells, exhaustion of engineered T cells, cancer cells' immune-evasion, and the lack of validated targets that are shared among most cancer-patients (30). A body of research is working towards finding solutions for these challenges.

2.2.3. TIL therapy

TILs are a subpopulation of lymphocytes that migrate into tumors to eliminate cancer cells. When TILs are isolated from cancer patients' tumors and expanded in vitro, the product is a T cell population targeting multiple antigens, which are often largely unknown.

As of April 2021, there were 73 TIL therapy agents in the cancer cell therapy pipeline and a 4% increase from 2020 (23). TIL therapy has been most successful in treating melanoma, which is based on the melanomas high mutational burden, that generates a high rate of neoantigens, and the ability to achieve a sustained antitumor reactivity (30). Unfortunately, most of epithelial cancers do not share these characteristics with melanoma and lack a high mutational burden. Current efforts are focused on expanding the TIL therapy to other cancer types and optimizing the synthetization of TIL products since it is difficult to extract TILs from poorly immunogenic tumors cells (22). It is also important to be able to select the most suitable subpopulation of TILs for expansion; it has been shown that in some cancers only a fraction of a TIL population is tumor-reactive (32) and that the expansion of tumor-infiltrating T cells result in novel clonotypes, instead of tumor-specific (33). Other challenges in TIL therapies include short in vivo persistence in the patient after reinfusion.

A solution to these challenges could be genetically modified TILs, called synthetic TILs, that could express ligands that increase TILs cytotoxic potential, chemokine receptors for chemokines secreted by cancer cells to improve the TIL migration toward tumors after reinfusion, and PD-1 knock-out TILs that would resist exhaustion (34). The authors speculate that with synthetic TILs, it could be possible to generate personalized TILs addressing the immune-evasion tactics present in the individual patient.

2.2.4 Therapeutic cancer vaccines

The principle of therapeutic cancer vaccines is that the vaccine delivers a tumor-specific antigen to APCs, which in turn activates both cytotoxic T cells and helper T cells, that will eliminate the tumor cells (35). The development of cancer vaccines has been hard, and despite a lot of research and trials, only two therapeutic cancer vaccines has been FDA-approved. With the advances in cancer immunobiology, it is now understood that the earlier vaccines have not been immunogenic enough to produce a clinical effect (36). Melief et al. (37) formulated that a successful cancer vaccine should deliver the antigen to activated dendritic cells, and activate the cells' cross-presentation pathway, which will lead to antigen presentation on both MHC class I and class II molecules, and therefore the dendritic cell will activate both cytotoxic T cells and helper T cells.

Another important consideration is the selection of an antigen. The optimal antigen can elicit a broad immune response and simultaneously avoid off-target effects on healthy cells. Current strategies aim for finding either shared tumor antigens or more personalized neoantigens. TAAs are autologous proteins that are shared among patients and have shown promise in late stage trials (36). TAAs limitation is that the autologous antigen can activate self-tolerance mechanisms that inhibit T cell activity, and result in elimination of T cells with high affinity to the TAA (37). The advances in genomics have enabled the study of neoantigens, that arise through genetic and epigenetic alterations in the cancer cells genome. Neoantigen are more likely to be different than the self-proteome and therefore neoantigens can avoid the problem of self-tolerance and possibly be more immunogenic. There are ongoing efforts to develop computational approaches that can predict which antigens result in the most efficient anti-tumor response (36).

2.3 Methods that assess T-cell receptor specificity

2.3.1 MHC multimer analysis

MHC multimers are soluble oligomeric forms of MHC monomers that are used to visualize antigen specific $CD8^+$ T cells *ex vivo*. The MHC multimers are loaded with a specific peptide and a fluorescent or metal label, which can be picked up with cytometry-based methods. The label can also be a DNA barcode, which can be collected by DNA sequencing. Applications of MHC multimer staining are the quantification and of antigen-specific T cells, enrichment of rare antigen-specific T cells, and single-cell classification (38). By combining MHC multimers with immunohistochemistry, the method can answer questions of T cell location, abundance and phenotype in situ (39).

To produce an unambiguous signal for flow cytometry, the T cell needs to bind numerous MHC multimers. Thus, T cells with low affinity to pMHC or low TCR expression may not obtain sufficient fluorescent signal intensity. The amount of fluorochromes that can be analyzed in one sample at the same time is limited due to available channels. Using combinatorial staining methods, 25 different T-cells have been detected in one sample. However, in combinatorial approaches the fluorochromes spectra are overlapping and need

compensation (38). This problem is avoided in mass cytometry where the labels are unique heavy metal ions. In mass cytometry there are more than 40 channels available and by using multiplex approach, it is possible to screen several hundred epitopes at the same time (40).

Another approach for screening T-cell specificity with large libraries of epitopes is the DNA barcode method, where one sample can be incubated with a collection of over 1000 MHC multimers. In this method, the marked cells are sorted, and the DNA barcode is amplified and sequenced, and the result is acquired by a retrospective analysis of the sequencing data that provides an estimate for T cell frequencies in the sample. The method is able to detect even low affinity TCR:pMHC interactions (41). Drawbacks of bulk analysis is that the information of individual T cell binding to peptides is lost. Other limitations of this approach are that the TCR sequences linked to the antigens cannot be obtained, and that the peptide synthesis is expensive and a time-consuming process (42).

To address these challenges, the tetramer-associated TCR sequencing (TetTCR-seq) has been developed. In this method a large library of fluorescently labeled and DNA-barcoded pMHC multimers is generated and presented to T cells. The stained cells are single-cell sorted and the genes of DNA-barcode and TCR are amplified by RT-PCR. Using a molecular identifier, the exact number of each species of tetramers bound to a T cell is obtained. Lastly, using nucleotide barcodes, TCR sequences are linked with bound peptide specificities (42).

The main disadvantage of multimer analysis is that the method requires determination of the MHC genotype of the examined individual before analysis. Other drawbacks are limited throughput of peptide synthesis, inefficiencies in the production of pMHCs, the instability of pMHCs, and that the visualized immune response may not be transferrable to other MHC molecules (39,43). In the DNA barcode approach users need to rely on good quality sequencing procedures and certified translation programs to acquire results (41).

2.3.2 Computational approaches studying T-cell receptor repertoires

The sheer number of antigens and TCRs calls for *in silico* approaches to handle the subject. Advances in high-throughput sequencing of TCRs and TCR:pMHC have called for ways to convert the obtained data to information about TCRs specificity to ligands. Approaches have

been developed to tackle this task and these analytical tools take large raw TCR sequence datasets and produce groups of TCRs which share epitopes. Using these programs, it is possible investigate a collection of TCR sequences and reduce a fraction of the sequences to groups with a meaningful antigen-specificity, and then these groups can be interrogated whether or not they are important in a biological scenario (44). Next, two articles from 2017, that are regarded as the seedling articles of the computational approaches, will be presented.

In their paper, Dash et al. (45) postulates that by utilizing the fact that TCRs from T cells that recognize the same antigen often have the same features in their conserved sequences, it could be possible to predict epitope specificity with an algorithm. In their article, they characterized over 4,600 in-frame single-cell-derived TCRαβ sequence pairs from 110 subjects and grouped them into ten epitope-specific TCR repertoires. The authors developed metrics that clustered and visualized the data into epitope specific TCR clusters that contained a group of TCRs with shared structural information, amino acid similarity and CDR lengths, and a dispersed set of varied outlier sequences. Next, the authors determined the shared motifs in the core TCR sequences and were able to underline the conserved residues that drive TCR recognition. In order to validate their method, the authors classified TCRs specific for influeza and were able to correctly predict their antigens.

In a parallel study, Glanville et al. (46) acquired sequencing data of over 2,000 TCRβ and paired αβ sequences from pMHC-tetramer sorted T-cells specific for eight different pMHC complexes, and together with structural data they determined the minimal requirements for TCR antigen specificity. They observed that in epitope-specific groups, TCRs shared enriched CDR3 sequences. Analysis suggested that these CDR3 sequences were likely to interact with the epitope. Based on these findings, the authors developed an algorithm, GLIPH, that produced clusters of TCRs with high probability of sharing epitope specificity on the basis of both conserved motifs and global similarities of CDR3 sequences. To validate their approach, they identified specificity groups in *Mycobacterium tuberculosis*-specific T cells and were able to map the HLA and peptide specificity of several of these groups. Additionally, the GLIPH-identified groups were used to successfully design artificial TCRs with experimentally validated binding specificity.

The experiments showed that it is possible to classify TCRs, that recognize the same antigen, into groups based on their shared structural features and sequence. By inverting this process,

TCRs can be grouped into clusters that can be used to predict their antigens (43,47). Leveraging the full potential of computational approaches has yet to be fulfilled since structural and functional data on the TCR:pMHC interface lag behind the scale of sequencing data, but increasing amounts of data are produced (48). Another bottleneck is the validation of TCR specificity and function *in vitro*. By having a high-throughput method for TCR specificity testing, the algorithms could be improved further, and one can postulate, developed to a point where we could take raw TCR sequencing data and do functional predictions (49).

2.3.3 Co-culture screens

Assessing T cell specificity is challenging since TCRs have relatively low affinity to their targets and antigens are small peptides that are non-covalently bound to MHC molecules. Additionally, antigen binding does not consistently lead to T-cell activation. For example, in yeast libraries where pMHC complexes are encoded by and presented on the surface of yeast for T cells to bind to, Sibener et al. (50) showed that TCRs high affinity to a pMHC complex does not equal a meaningful interaction *in vivo.*

Functional avidity is dependent on many factors: the expression level of TCRs, the quantity of pMHC complexes present on the surface of APCs, the amount of co-stimulatory molecules associated with the TCR, and the T-cells functional state. In co-culture approaches, many of these variables can be tuned or fixed in a way that enables us to directly compare TCRs specificity to an antigen (51).

Different co-culture approaches have been developed to assess TCR functional antigen recognition on a single-cell level. T-Scan (52) is a high-throughput platform for screening T-cell activating antigens from a cell-based library of pMHC complexes. The target cells express lentivirally-delivered candidate antigens, that are endogenously processed and presented on MHC molecules. T cells of interest are co-cultured with target cells and T-cell activation is assessed by monitoring a fluorescent reporter of granzyme B in the target cell, which is a cytotoxic molecule that activated T cells secrete to their target cells. Cognate antigens are sorted by fluorescence-activated cell sorting (FACS), amplified with PCR and

identified with next-generation sequencing. The limitation of this method is that candidate antigens need to be genetically encoded, which prevents the mapping of some post-translational modifications and non-peptide antigens.

Another approach developed by Paria et al. (53) is a non-viral and non-next-generation sequencing platform, which identifies TCRs that are activated by cognate antigens. This method combines TCRαβ gene synthesis and in vitro-transcribed mRNA, and therefore avoids the time-consuming conventional method of producing TCR-encoding retroviruses. First, T-cells of interest are co-cultured with dendritic cells that present antigens. Then, using single cell sorting, RT-PCR and Sanger sequencing, the reactive TCRs are found. Then, the TCR is reconstructed by in vitro-transcribed-TCR-mRNAs, that are used to transfect Jurkat luciferase cells with TCRs of interest. Finally, TCR stimulation is determined by monitoring either cytokine production or a NFAT promoter reporter.

Lastly, Hu et al. (51) presents a co-culture screen, where a variable chain plasmid library was used to clone TCRs and transferred into a lentiviral vector. Next, the reconstructed TCR was expressed in a reporter cell line, which in turn were co-cultured with an APC that presents a candidate antigen. The specificity and activation of the reporter cell line were detected based on IL-2 secretion, the expression of CD69, or luciferase activity. Then, the authors applied this system to find neoantigen-specific TCRs from melanoma patients that were treated with personalized neoantigen vaccines. The TCRs were discovered by single-cell sequencing. In 9 days, they were able to make TCR-expressing reporter cells that were reactive against the neoantigen mut-MGA.

These co-cultures, where engineered APCs present antigens to TCR reporter cells, could be used as an indicator of how T cells will recognize potential tumor targets. It is also possible to assess strategies to increase the response of transferred T cells, e.g., by overexpressing tumor-specific co-stimulatory proteins (54). By scaling up the screen it is possible to generate functional TCR-specificity data, that would solve the bottleneck of lacking functional data in the development of predictive algorithms for TCR-recognition.

3 Experimental part

3.1 Introduction and aims

Here, we will present the work we did towards setting up a Jurkat-based co-culture screen that assesses TCR specificity and functionality. Our starting materials are Jurkat reporter cell lines and K562 cell lines that are a kind gift from Peter Steinberger's group in University of Vienna. The Jurkat reporter cells are modified human Jurkat cells E6.1 that are devoid of endogenous TCRα- and β-chains and have triple parameter reporter (TRP cells) or single reporter (NFAT cells) upon TCR activation (55). These cells can be engineered to express selected human TCRs, and When these cell lines' TCRs binds to their cognate antigen presented by an APC, response elements to the transcription factors NF-κB, NFAT and AP-1 drive the expression of the fluorescent proteins CFP, eGFP and mCherry respectively (54).

These cells can be used to test the cells' antigen-specific responses by coculturing them with tumor cell lines that expressed the antigens of interest endogenously, or with peptide loaded cells. Müller et al. (49) produced corresponding triple parameter reporter knockout (TRP^{KO}) cell lines. They investigated the TRP^{KO} cell lines' suitability for high-throughput TCR functional testing by re-expressing 59 human TCRs in the cells and characterized their antigen specificity and functional avidity. They performed parallel experiments with primary human T cells for direct comparison. The authors came to the conclusion that TRP^{KO} cell lines' pMHC-multimer stainability and functional avidity were almost identical with the primary T cells, and therefore suited for cellular platforms for TCR testing. Additionally, TRP^{KO} cell lines have almost an indefinite ability to expand and therefore is easier to maintain a fixed repertoire of TCR-expressing cells.

In our screen we will co-culture the Jurkat reporter cells with artificial APCs (aAPCs), the K562 based cell lines that have a stabilized HLA-A2. Additionally, and one of the two K562 cell lines have a stabilized CD86. Our starting materials also include lentiviral plasmids that will be used to transfect the Jurkat reporter cells with a synthetic TCR. The envelope plasmid pMD2, packaging plasmid psPAX2 and transfer plasmid N103 are a kind gift from Mark Davis group in Stanford University. The envelope plasmid codes for the virus envelope, the

packaging plasmid codes for packaging the viral particles and the transfer plasmid will contain the insert, and code for TCRα and TCRβ.

The workflow of our screen is presented in figure 4. The workflow starts with single-cell sequencing data of paired TCRαβ chains that reveals detailed data of the CDR3 region and enables the reconstruction of the TCR. Next, the TCRαβ chains are cloned into lentiviral vectors and a viral supernatant is produced. This supernatant can be used to infect the Jurkat cell lines. Now, the Jurkat cells express the TCRαβ chains of interest and they can be co-cultured with engineered APCs that present candidate antigens on MHC molecules. The co-culture is subsequently analyzed with flow cytometry, with a positive signal of T-cell activation is detected, and thus the functional avidity of the reconstructed TCR is assessed in a streamlined and controlled system.

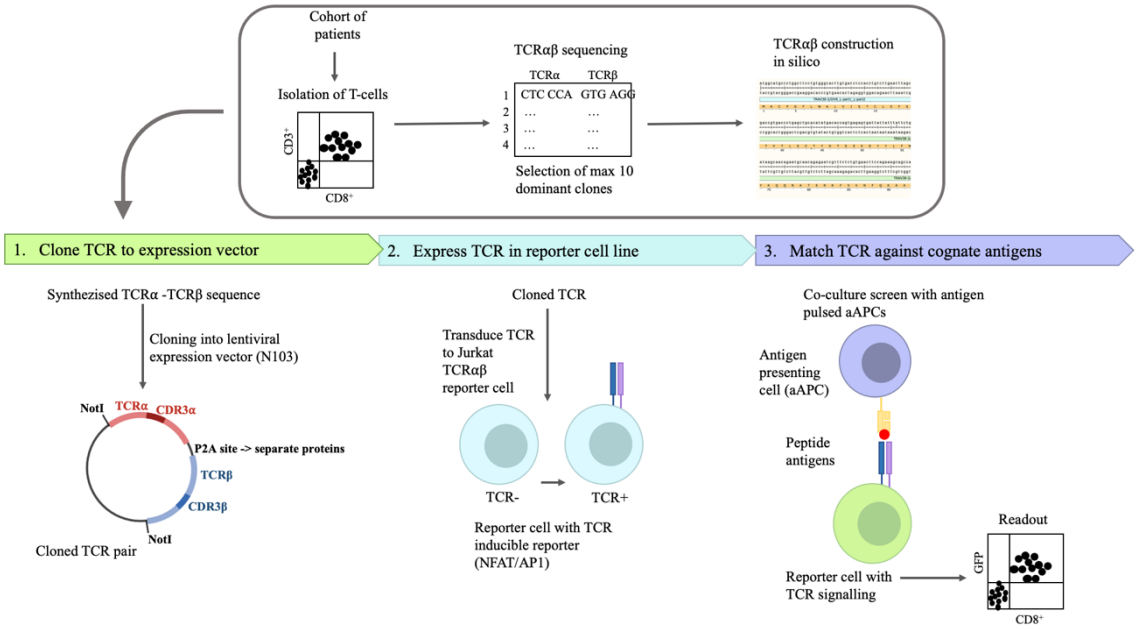

Figure 4. Workflow of co-culture screen. The workflow starts with single-sequencing data of interesting TCRs, which are reconstructed in silico. Then, (1) the synthesized TCR is cloned into a lentiviral vector, which will be used to (2) express the synthetic TCR in reporter cells. Now, (3) reporter cells can be co-cultured with aAPCs and the TCR specificity and T-cell activation can be measured with flow cytometry. Figure is inspired by Hu et al. (51).

Our aim is to work toward setting up the screen by successfully cloning a reconstructed TCR into the vector plasmid, characterize the Jurkat reporter cell lines and K562 cell lines, and optimizing a flow cytometry set up for analyzing the activated Jurkat reporter cell lines.

3.2 Methods

3.2.1 Amplification of TCRα and TCRβ by PCR

For the synthesis of our vector plasmid, we amplified our inserts with long overlaps required for Gibson assembly by PCR. Our inserts, the synthetized TCRα and TCRβ sequences of A6, and corresponding forward and reverse primers, were ordered from Integrated DNA Technologies and reassembled in Elution Buffer BE (#740306.100, Macherey-Nagel). The PCR reaction presented in table 1 was prepared.

Table 1. Reaction mixture for TCRα and TCRβ amplification.

Reagent	**Amount**
Phusion DNA Polymerase (#F-530L, Thermo Scientific)	0.25 µl
5X Phusion HF Buffer (#F-518, Thermo Scientific)	5.0 µl
10 µM forward primer	1.25 µl
10 µM reverse primer	1.25 µl
10 mM dNTP Mix (#R0192, Thermo Scientific)	0.5 µl
Template DNA 1 ng/µl	1.0 µl
Nuclease-Free Water (#AM9937, Life Technologies)	to 25 ul

Seven PCR reactions was prepared for TCRα and TCRβ, and one negative control each, in which all other reagents were added except the template DNA. The PCR reaction mixtures were cycled through the conditions presented in table 2 using the T100^{TM} Thermal Cycler (BioRad).

Table 2. PCR reaction cycles.

Step	Cycles	Temperature	Time
Initial denaturation	1	98°C	30 s
Denaturation	30	98°C	10 s
Annealing		70°C	30 s
Extension		72°C	30 s
Final extension	1	72°C	10 min
Hold	1	4°C	∞

3.2.2 Agarose gel electrophoresis: evaluation and purification of PCR products

For evaluation of PCR products, we used the standard agarose type LE (#BN-50004, Bionordika), and for purification of PCR products we used the low gelling temperature agarose type VII-A (#A0701-25G, Sigma-Aldrich). Midori Green (#MG04, Nippon Genetics Europe) was added to the 0.8% gels for in-gel staining of DNA. Samples were loaded to the wells mixed with gel loading dye (#B7024A, New England BioLabs). We used the 100 bp DNA ladder (#N3231S, New England BioLabs) or the 2-Log DNA ladder (#N3200S, New England BioLabs) depending on the sample size. Samples were run using the PowerPac™ Basic (BioRad) with 100 V until the needed separation was achieved. Blots were imaged with the ChemiDoc™ MP Imaging System (BioRad).

We purified our PCR product by running the samples through the agarose gel and collecting the bands containing the PCR product. To separate the DNA from the agarose gel, we used the NucleoSpin TriPrep Mini kit for RNA, DNA, and protein purification kit (#740966.50 Macherey-Nagel). DNA concentration was measure with NanoDrop™ 2000 (#ND-2000, ThermoFisher Scientific).

3.2.3 Plasmid assembly

The TCRα, TCRβ and vector plasmid N103 was assembled with the NEBuilder® HiFi DNA Assembly Cloning kit (New England BioLabs). For the assembly reaction we used 100 ng of the digested vector plasmid N103, and a 2-fold molar excess of TCRα and TCRβ. We added 10 µl of NEBuilder HiFi DNA Assembly Master Mix (#M5520A, New England BioLabs) and finally added nuclease-free water (#AM9937, Life Technologies) up to 20 µl. As the positive control we used the NEBuilder Positive Control (#N2611A, New England BioLabs), and as the negative control we took a sample of the assembly reaction mixture before incubating. The assembly reaction mixtures were incubated for 15 minutes at 50°C, after which we took a sample. We continued to incubate the reaction mix up to 60 minutes at 50°C and took another sample. The assembled plasmids were then transformed to One Shot Stbl3™ Chemically Competent Cells (#C7373-03, Invitrogen by Thermo Fisher Scientific).

3.2.4 Restriction enzyme digestion of PCR and assembly products

To evaluate if the plasmid assembly has succeeded, we digested the plasmids with the restriction enzymes EcoRI (#3101S, NewEngland BioLabs) and NotI (#R3189S, NewEngland BioLabs). Table 3 presents the digestion mixture that was prepared.

Table 3. Reaction mixture for restriction enzyme digestion.

Reagent	**Amount**
DNA	0.5 µg
CutSmart5X	2.5 µl
EcoRI	0.5 µl
NotI	0.5 µl
H2O	To 25 µl

3.2.5 Transformation

We chilled 5 ng of the assembled plasmid and added it to a vial of Stbl3 cells and placed the mixture on ice for 30 minutes. Then we heat shocked the cells at 42°C for 45 seconds and placed the vial on ice for 2 minutes. Room temperature SOC media was added to the tubes and mixture was shaken at 225 rpm, 37°C for 60 minutes. Next, 50 µl of the mixture was spread onto pre-warmed LB plates with 100 µg/ml amplicin, and incubated overnight at 37°C.

Following day colonies were chosen and sub-cultured in 5 ml LB-medium with 100 µg/ml ampicillin. Cultures were incubated overnight at 37°C and 250 rpm. Next, cultures were scaled up by diluting 1/1000 of the culture in 100 ml LB-medium with 100 µg/ml ampicillin and incubated overnight at 37°C and 250 rpm. Finally, we purified our assembled plasmids using NucleoBond Xtra Midi EF, Midi kit for endotoxin-free plasmid DNA (#740420.50, Macherey-Nagel).

3.2.6 Sanger sequencing of TCRα and TCRβ in the assembly product

Further analysis of the success of the plasmid assembly was performed using the SeqLab sequencing service at the FIMM Institute for Molecular Medicine Finland. The purified plasmids were combined with primers for sanger sequencing (Table 4 and 5). We wanted to sequence the TCRα and TCRβ regions separately and therefore both TCRα and TCRβ were supplied with one forward and one reverse primer each. Samples with primers were sent to FIMM where the samples were purified, electrophoresis was run with ABI3730xl DNA Analyzer and basecalling with Sequencing Analysis 5.2 was performed. The results were delivered in FASTA format which we aligned with our reference sequence using NCBI BLAST search tool to evaluate the plasmid assembly.

Table 4. Reaction mixture for sanger sequencing.

Reagent	**Amount**
Template DNA	1.0 µl
Primer	1.6 µl
Nuclease-free H2O	4.0 µl
Vtot	6.6 µl

Table 5. Amount of DNA that was used for sanger sequencing.

Clone	**Amount (ng)**
1	665
4	797
5	599
9	779
10	436

3.2.7 Cell culture

The Jurkat reporter T cell lines (Jurkat TRP and Jurkat NFAT), parental Jurkat cell line, the K562 cell lines (K562 and K562_CD86), and parental K562 cell line were cultured in RPMI Medium (#72400, Gibco) with 10 % Foetal Bovine Serum (FBS) in an incubator with the conditions 37°C and 5% CO_2.

3.2.8 Flow cytometry analysis of protein expression

The cells were prepared for flow cytometry analysis by taking 5 x 10^5 cells per staining from 80-90% confluent cultures. The cells were washed with PBS (#21-040-CV, Corning) before staining with monoclonal antibodies for 15 min in darkness. The monoclonal antibodies listed in table 6 were used to study surface protein expression on the cell lines. After another wash with PBS, cells were suspended in 500 µl PBS and ready for the flow

cytometry analysis performed using BD FACSVerse™ (BD Bioscience). During flow cytometry analysis 100 000 events was acquired per sample.

Table 6. Fluorochrome markers used in flow cytometry analysis.

Marker	**Fluorochrome**	**Catalog number**	**Provider**
CD125	APC	560938	BD Pharmingen
CD28	BV510	56075	BD Bioscience
CD3	APC-H7	560275	BD Pharmingen
CD8	PE	60022PE	Stem cell
CD80	BV510	563084	BD Pharmingen
CD86	PerCP-Cy5.5	561129	BD Pharmingen
HLA-ABC	PE-Cy7	561349	BD Pharmingen
HLA-A2	PE	55870	BD Biosciences
TCRαβ	APC	306718	BioLegend
TCRαβ	FITC	333140	BD Biosciences

3.2.9 Activation experiment with Jurkat based reporter cells

When T cells are treated with phorbol 12-myristate 13-acetate (PMA), that is an analog of DAG, and ionomycin, that forms pores in the cell membrane and enables Ca^{2+} influx, the T cell is driven to a state that largely reconstitute the effects of T-cell activation[1].The functional basis of reporter cells is that when the cells are activated, they display a fluorescent marker. We stimulated the cells with PMA and ionomycin with different concentrations for 24 hours, after which the protein expression was analyzed with flow cytometry.

From an 80-90% confluent cell culture, 5 x 10^5 cells were collected and distributed on a 12 well plate and incubated in cell culture conditions over night. Next, 1 µM PMA and a concentration series of ionomycin (1 µM, 3 µM, 6 µM, 9 µM) was added to the wells and incubated for 24 hours. Finally, the stimulated cells were collected, washed with PBS and reporter expression was analyzed by flow cytometry.

3.3 Results and discussion

3.3.1 Amplification of TCRα and TCRβ

For the purpose of optimizing the screen, we used the well characterized human TCR A6, that is specific for human T-lymphotropic virus type 1 Tax peptide and bind to HLA-A2 (56). Synthetized TCRα and TCRβ sequences of A6 were amplified by PCR. To evaluate the success of the amplification, the PCR product was run through an agarose gel. The TCRα (866 bp) showed two bands: one more prominent band representing the TCRα and a weaker band representing some side product (Figure 5A). The side product may be a result of an uncomplete binding of a TCRα side chain, or the primer might partially bind to the wrong position and result in a side product. Moving forward, we will separate the correct TCRα from the side product by running the PCR product through an agarose gel and cut the TCRα out. TCRβ (987 bp) showed one band representing a PCR product only containing the TCRβ (Figure 5B), therefore the amplification was successful, and the PCR product can be directly used for plasmid assembly.

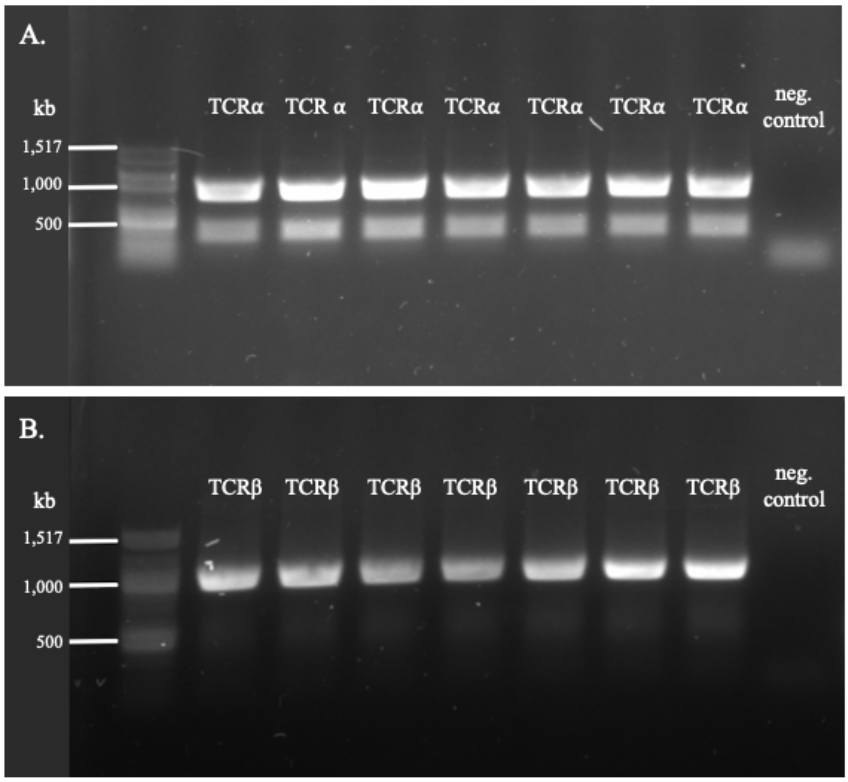

Figure 5. Amplification of TCRα and TCRβ, For TCRαβ synthesis we amplified synthetic TCRα and TCRβ-chains by PCR. As negative controls (neg. control) we used PCR reaction product that was prepared without the template DNA. (A) TCRα (866 bp) showed two bands: one just under 1,000 bp and another under 500 bp. (B) TCRβ (987 bp) showed one band just under 1,000 bp.

3.3.2 Assembly of vector plasmid

We assembled vector plasmids by Gibson assembly, where the amplified TCRα (866 bp) and TCRβ (987 bp) sequences are combined with the vector plasmid N103 (8644 bp). In the reaction mixture, the primers will facilitate the 5´exonucleases synthetization of long overhangs in the ends of the different sequences, that in turn will guide the correct assembly order. Then, DNA polymerase fills the gaps of the annealed single strand regions and DNA ligase seals the nicks. Next, the assembled vector was transformed into Stbl 3 *Escherichia coli*. The background sample, that was a reaction mixture sample obtained before incubation, had 27 colonies after an overnight incubation. Both positive controls, that were provided in

the reaction kit, had over 150 colonies (Table 7), which indicates that the assembly and transformation was successful. The Gibson assembly produced 47 colonies when the 15 min incubation was used, and 49 colonies with the 60 min incubation. Since the number of colonies were similar, the assembly did not seem to need the longer incubation time and therefore in upcoming experiments we could only use the 15 min incubation.

Table 7. The number of transformed *E.coli* colonies.

Sample	Number of colonies
Negative control, no bacteria	0
Gibson background	27
Gibson 15 min	47
Positive control 15 min	> 200
Gibson 60 min	49
Positive control 60 min	> 150

10 colonies were selected for further growth: 5 from 15 min incubation and 5 from 60 min incubation. After an overnight incubation, the plasmid DNA was purified from the *E. coli* colonies and digested with the restriction enzymes EcoRI and NotI, which separated the N103 (8644 bp) and the insert TCRαβ (1853 bp). When the digested plasmid was run through an agarose gel, the successfully assembled plasmids appeared as two bands at 8.0 kb and at 1.8 kb resembling N103 and TCRαβ respectively (Figure 6). The clones 1, 4, 5, 9 and 10 were equipped with both TCRα and TCRβ, which indicates that 50 % of the selected colonies had successfully produced the assembled vector plasmid. This was a good success rate and the clones with the assembled plasmid were chosen for further sequencing analyses.

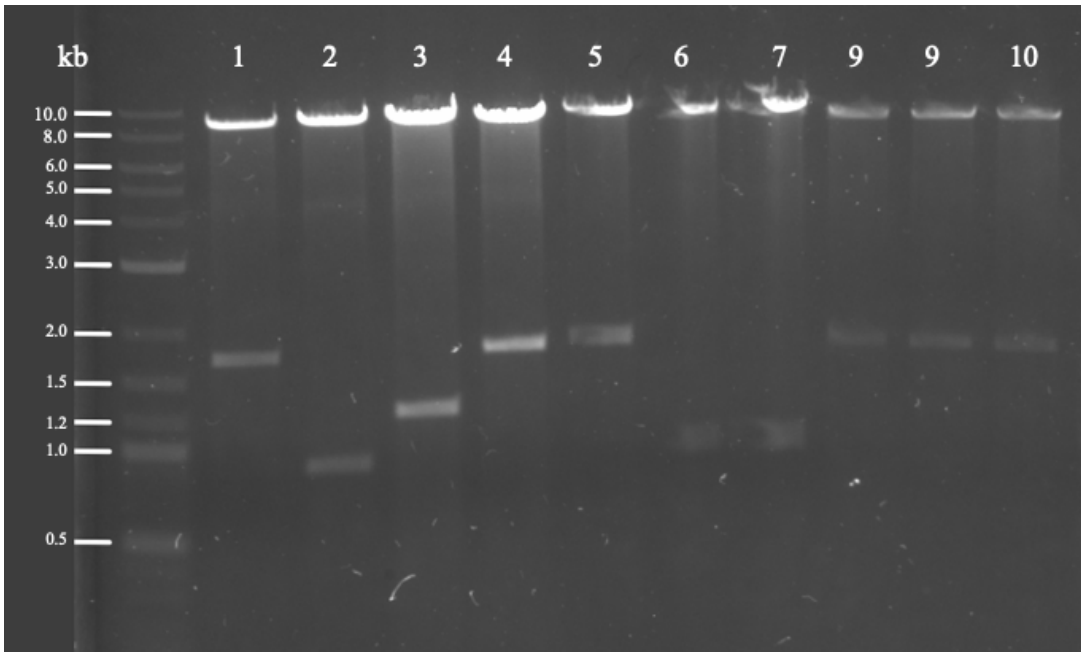

Figure 6. Clones of assembled N103_A6 plasmid. The assembled plasmids were digested with restriction enzymes and run through an agarose gel. A successful assembly includes the vector plasmid N103 (8,644 kb) and the insert TCRαβ (1.853 kb), which the clones 1,4, 5, 9, and 10 presents. Numbers over wells indicate the clone number.

3.3.3 Sanger sequencing of TCRα and TCRβ in the assembled plasmid

To further evaluate the success of plasmid assembly, the TCRαβ region was analyzed by sanger sequencing. We used separate forward and reverse primers for both TCRα and TCRβ. The sanger sequencing data was aligned with the original A6 TCRαβ sequence using NCBI BLAST, which revealed gaps in the sequences of clones 1, 4, 5 and 10, as well as an insert and a mismatch in clone 4 (Figure 7).

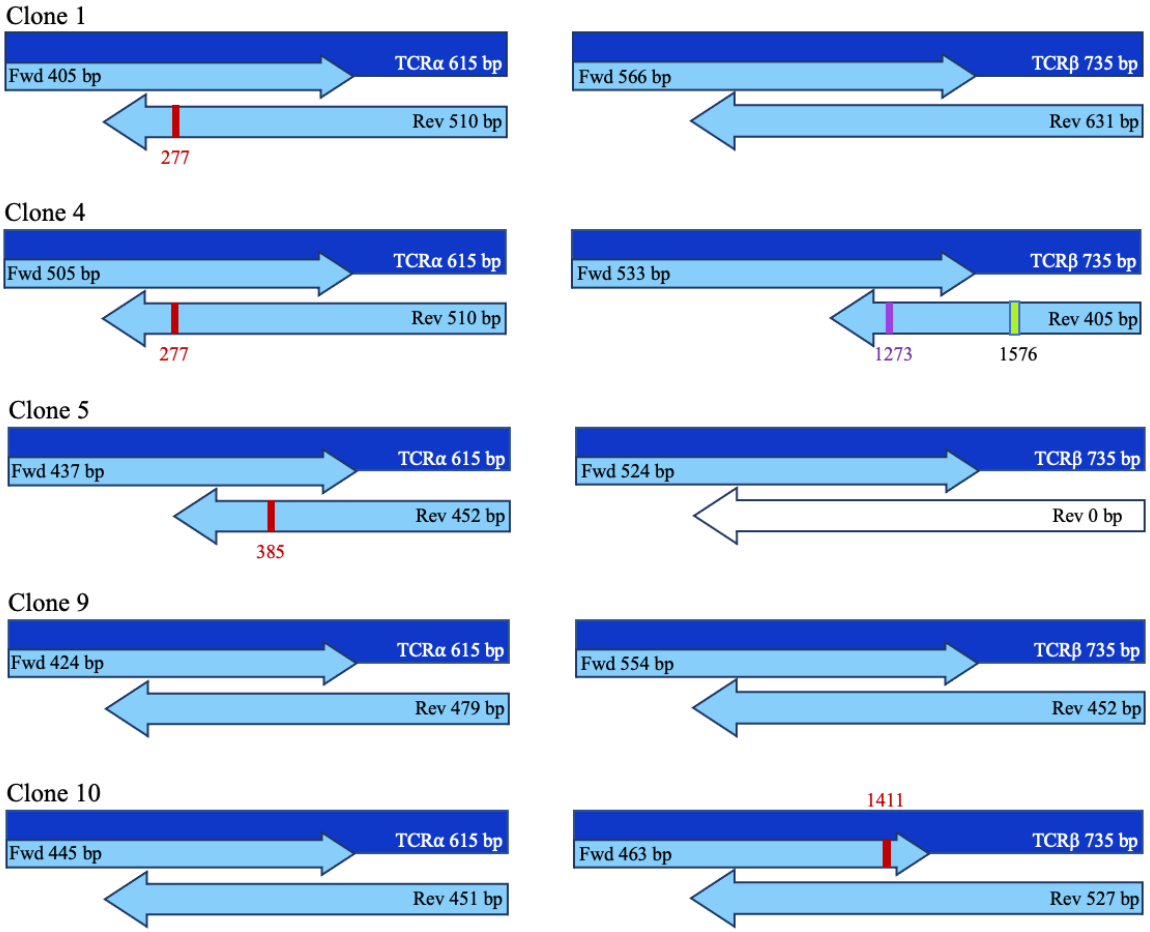

Figure 7. Overview of sanger sequencing results. In the sanger sequence analysis, we used separate forward (Fwd) and reverse (Rev) primers for TCRα and TCRβ. The sequencing data was aligned with the corresponding TCRαβ sequence using NCBI BLAST. The dark blue rectangle represents the original TCRα and TCRβ sequence, light blue arrows represent the aligned sanger sequencing data, and the red, violet and green lines represent gaps, insertions and mismatches respectively. The white arrow indicates that the sequence was not analyzed.

The unwanted defects in the sequences could be a result of some inconsistency in the experiments or weak sample quality. When looking at an example excerpt of the sequencing chromatogram (Figure 8), where good quality samples was indicated as a light blue color in the upper row, and high, thin peaks in the lower row, we could see that the overall quality of the samples was weak since the upper row had a lot of dark blue nucleotides and low, wide peaks. When the sample quality was weak, we believe that some nucleotides were interpreted

as gaps, inserts and mismatches. Going forward, the sample quality could be improved by having a higher template concentration in the samples and using new primers.

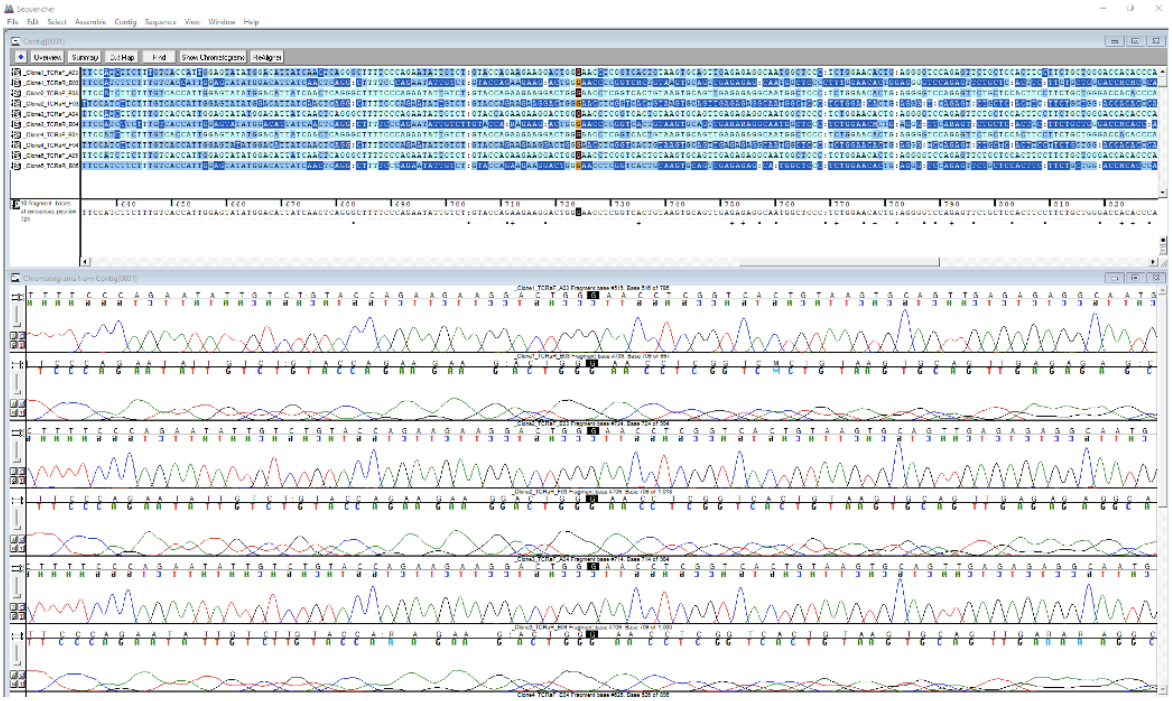

Figure 8. Excerpt of a chromatogram of an TCRα chain. In the upper row, the light blue nucleotides represent a better sample quality and dark blue bad sample quality. In the chromatogram, higher and thinner peaks indicate a strong signal of a nucleotide, whereas lower and wider peaks indicate a weak signal.

3.3.4 Characterization of the Jurkat based reporter cell lines

We characterized the Je6.1 TRP and Je6.1 NFAT cell lines using flow cytometry. As a control we used a parental Jurkat cell line. FlowJo software (version 10.8.1) was used for data analysis and RStudio (version 1.4.1717) and ggplot2 was used for making bar plots. In our gating strategy (Figure 9) we used the unstained parental sample for gating. First, using an FSC-H vs FSC-A plot, we gated single cells from doublets and copied the selection to all samples. Next, from the single cell gate, a subset of cells was selected, and the gate was copied to all samples. Finally, working with one fluorochrome at a time, we gated the positive signal area based on the unstained control.

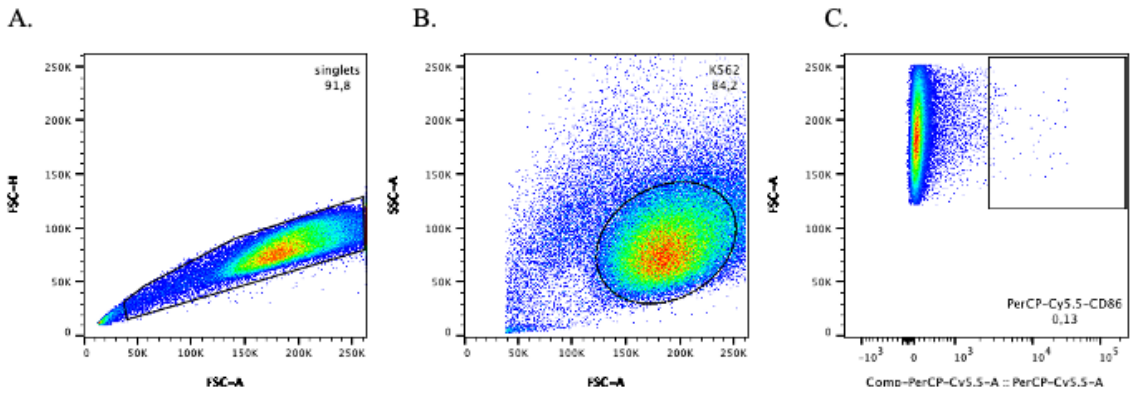

Figure 9. Gating strategy in flow cytometry data analysis. (A) The singlets were selected from an FSC-H vs FSC-A plot. (B) Using the previous gate, the cell population of interest is selected using an SSC-A vs FSC-A plot. (C) In a plot with a selected fluorochrome on the x-axis and FSC-A on the y-axis, the positive signal area was gated using the unstained control.

Figure 10 presents the expression of TCRαβ. In the reporter cell lines Je6.1 TRP and Je6.1 NFAT, TCRαβ has been knocked-out and we assumed that there would not be any TCRαβ expression. A parental Jurkat cell line, with its endogenous proteins intact, was used as a positive control. The percent of cells inside the positive signal gate in the unstained parental Jurkat cell line was 0.29% and stained parental Jurkat cell line 30.6%. We had expected a larger percentage of the population to be positive. The weak signal may indicate a low surface expression of TCRαβ in the parental Jurkat cell line or a compromised reagent. The corresponding percent of cells in the Je6.1 TRP samples were 1.28 x 10^{-3} % and 0.22%, and in the Je6.1 NFAT samples 0.28% and 5.05%. These percentages indicate that the reporter cell lines do not express TCRαβ and are therefore suitable for re-expression of a synthesized TCRαβ.

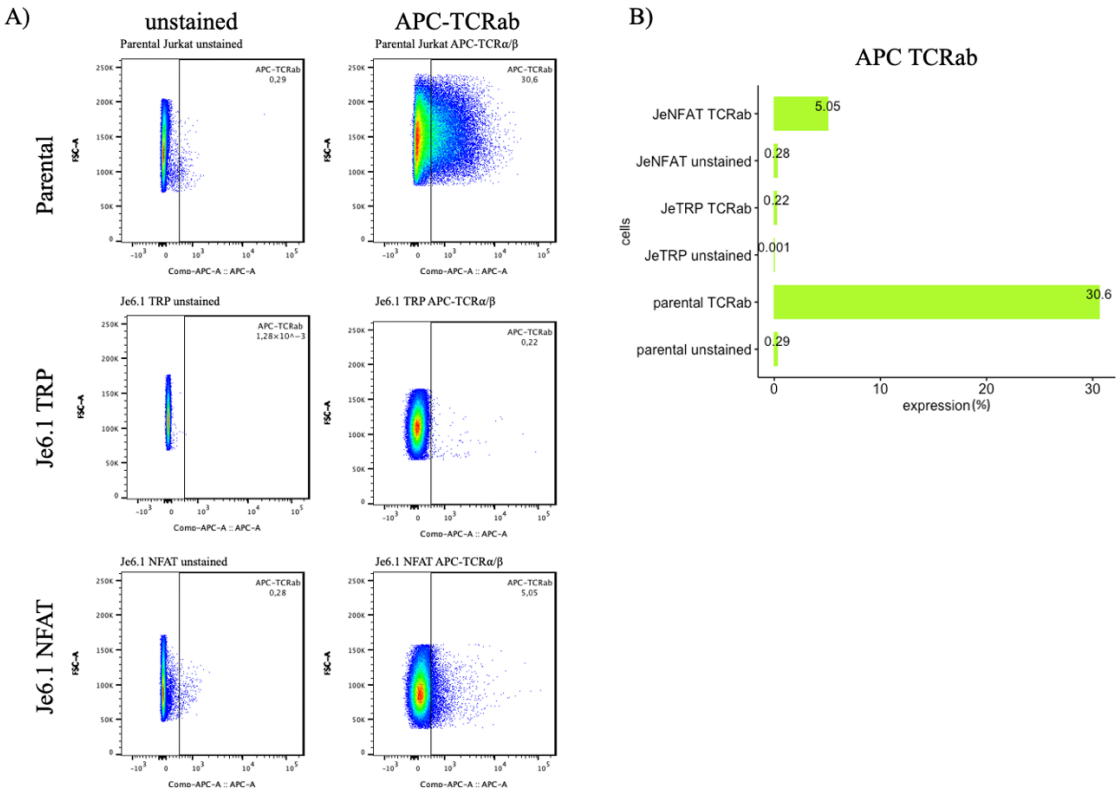

Figure 10. The TCRαβ expression in Je6.1 TRP, Je6.1 NFAT and parental Jurkat cell line. (A) Dot plot representation of the TCRαβ expression in the parental Jurkat, Je6.1 TRP and Je6.1 NFAT cell lines. Parental Jurkat cell line was used as a positive control and showed an expression of endogenous TCRαβ. However, TCRαβ has been knocked-out from Je6.1 TRP and from Je6.1 NFAT cell lines, and neither of the reporter cell lines expressed TCRαβ. (B) Bar plot representation of the TCRαβ expression in the stained and unstained cell lines.

Figure 11 represents the expression of CD3 in our cell lines. Our positive control, the parental Jurkat cell line, the percentage of positive cells was 0.25% in the unstained sample and 67.6% in the stained sample, and therefore the cell line was equipped with CD3. The corresponding percentages in our reporter cell lines were 0.043% and 56% in the Jurkat TRP cell line, and 0.13% and 31.5% in the Jurkat NFAT cell line. CD3 is stabilized when TCR is expressed, and therefore we assumed that the parental Jurkat cell line has the strongest CD3 expression. When we look at the dot plot of the Jurkat reporter cell lines, it seems like there is one cell

population in the frame below the positive signal area, and another cell population with a very strong signal outside the plot. The first population might be a dead cell population, and another staining experiment could be done to collect the cell population that potentially emit a stronger signal.

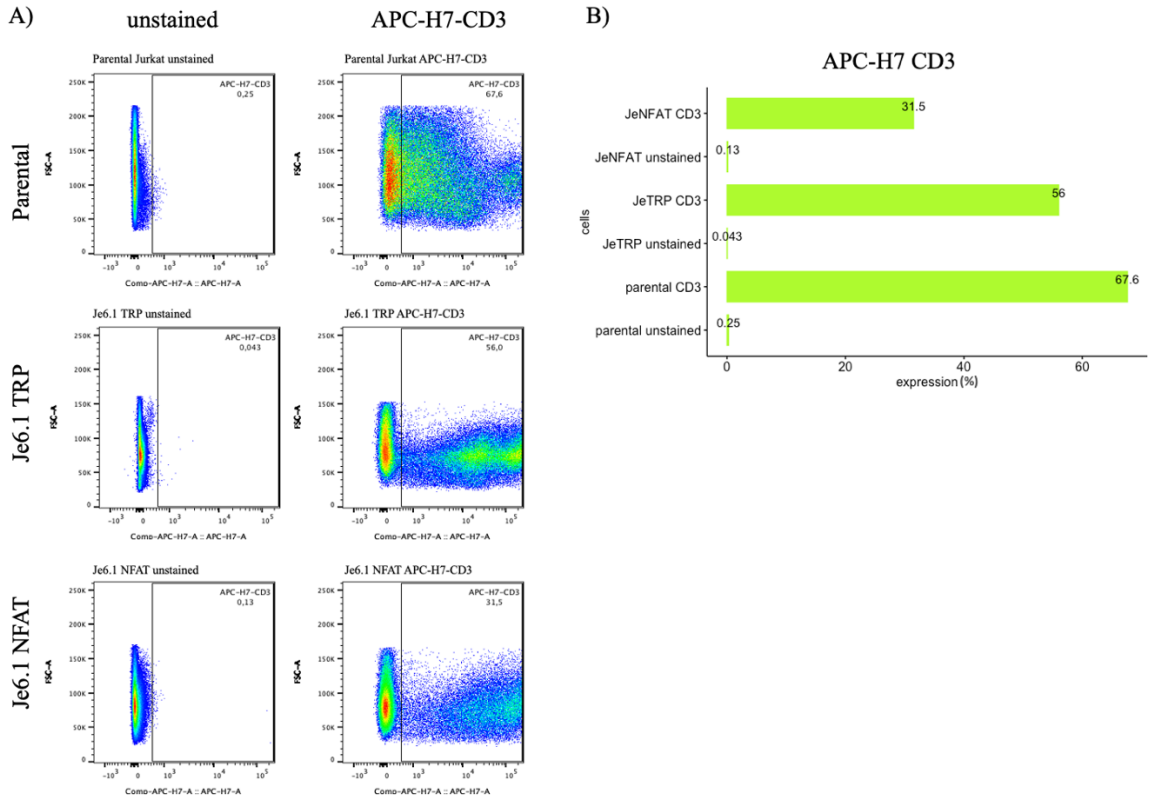

Figure 11. The CD3 expression in Je6.1 TRP, Je6.1 NFAT and parental Jurkat cell line. (A) Dot plot representation of CD3 expression. The parental Jurkat cell line was equipped with CD3. In both Je6.1 TRP and Je6.1 NFAT there was a CD3 expression, but not as strong as in the positive control. (B) Bar plot representation of CD3 expression.

Figure 12 presents the expression of CD8 in the Jurkat cell lines. In the parental Jurkat cell line the percentage of positive cells in the unstained sample was 0% and in the stained 10.3%. In the Jurkat TRP cell line, the corresponding percentages were 0% and 58.7%, and in the Jurkat NFAT cell line 0% and 59.3%. The results indicate that the proximally half of the reporter cell population expressed CD8. The next step could be to sort the CD8 positive cells and continue the experiment with them.

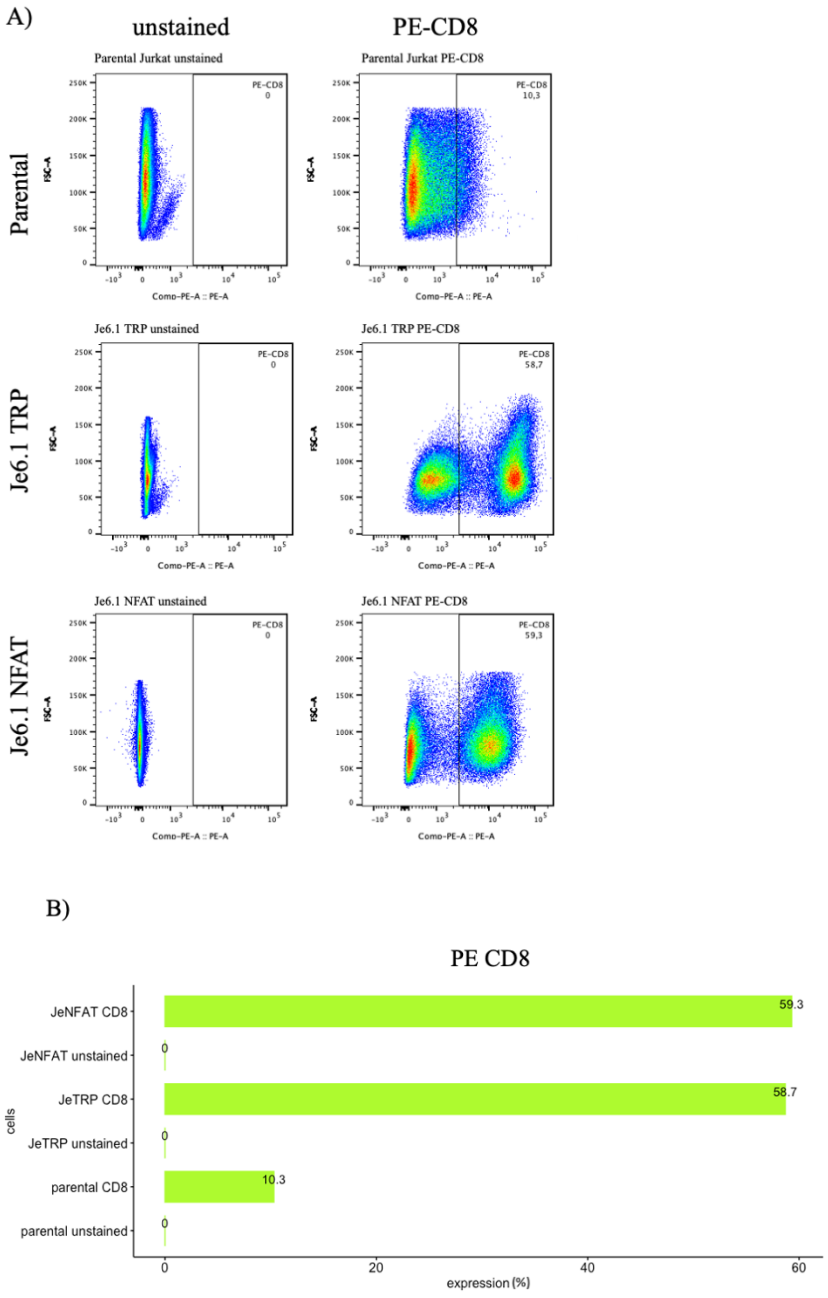

Figure 12. The CD8 expression in Je6.1 TRP, Je6.1 NFAT and parental Jurkat cell line. (A) Dot plot representation of the CD8 expression. The parental Jurkat cell line does not express CD8 and the plot represents background signal. The Je6.1 TRP and Je6.1 NFAT cells formed two separate populations, where proximally 50% of the cell population expressed CD8. (B) Bar plot representation of the CD8 expression.

Figure 13 represents the CD28 expression in Jurkat cell lines. The percent of cells inside the positive signal gate in the unstained parental Jurkat cell line was 16.1% and stained parental Jurkat cell line 77.0%. In the Jurkat TRP cell line, the corresponding percentages were 0.46% and 8.03%, and in the Jurkat NFAT cell line 1.38% and 42.8%. The CD28 expression is essential for T-cell activation and therefore a higher expression would be optimal. However, the CD28 expression might be upregulated when the reporter cells get a synthetic TCR.

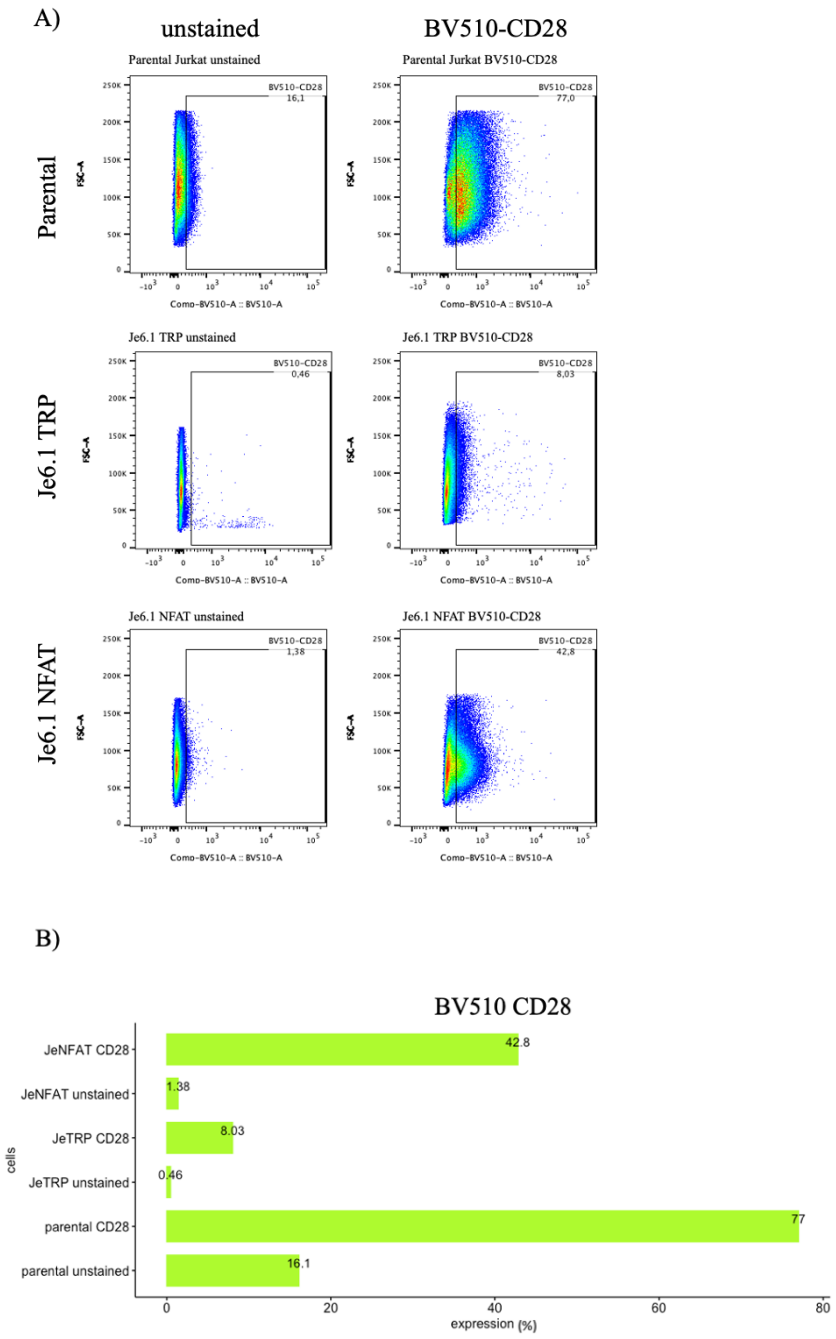

Figure 13. The CD28 expression in Je6.1 TRP, Je6.1 NFAT and parental Jurkat cell line. (A) The parental Jurkat cell line was used as a control in the analysis of CD28 expression, and the cell line was equipped with CD28 that plays a role in T-cell activation. The CD28 expression in the Je6.1 TRP (B) and in the Je6.1 NFAT (C) cell lines were weaker compared with the parental cell line.

In figure 14, the expression of CD152, or CTLA-4, is presented. CD152 competes with CD28 and inhibits T-cell activation. The percent of parental cells in the positive gate in the unstained sample was 4.67% and in the stained sample 4.62%. The corresponding percentages in the Jurkat TRP cell line were 1.26% and 3.39%, and in the Jurkat NFAT cell line 9.49% and 7.55%. The results indicate that the cells do not have a stabilized CD152 expression that could inhibit T-cell activation in later experiments.

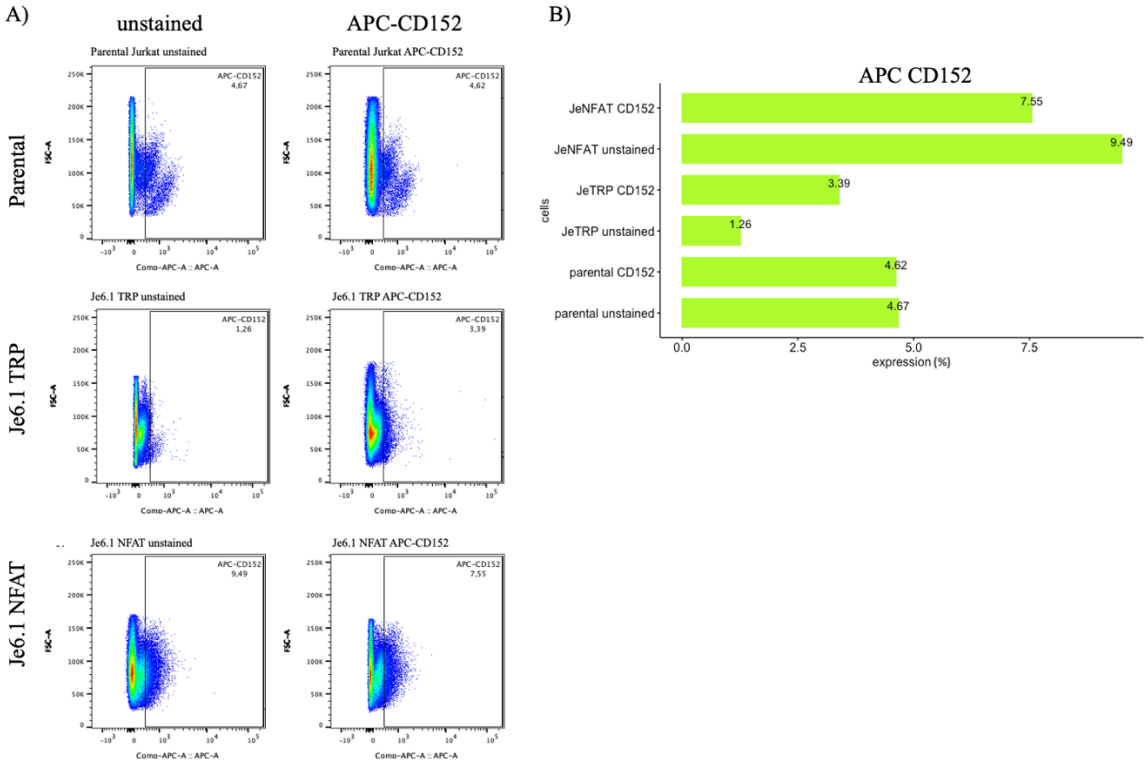

Figure 14. The CD152 expression in Je6.1 TRP, Je6.1 NFAT and parental Jurkat cell line. (A) Dot plot representation of CD152 expression. The parental Jurkat cell line did not show an expression of CD152 that is related to T-cell inactivation and competes directly with CD28. Neither did Je6.1 TRP or Je6.1 NFAT cell lines express CD152. (B) Bar plot representation of CD152 expression.

3.3.5 Characterization of the K562 based cell lines

We characterized the K562 and K562_CD86 cell lines by analyzing the expression of HLA-A2 and CD86 using flow cytometry. Our aAPC cell lines has a stabilized HLA-A2 and therefore we assumed that they express the protein (Figure 15). As our negative control we used the parental K562 cell line, the percentage of the positive cell population was 0.20% in the unstained sample, and 0.26% in the stained sample, which indicates no HLA-A2 expression. The corresponding percentages in the K562 cell line was 0.13% and 98.3%, and in the K562_CD86 cell line 0.27% and 98.9%, which indicates that both aAPC lines have a successfully stabilized HLA-A2 expression and are suitable for our experiments.

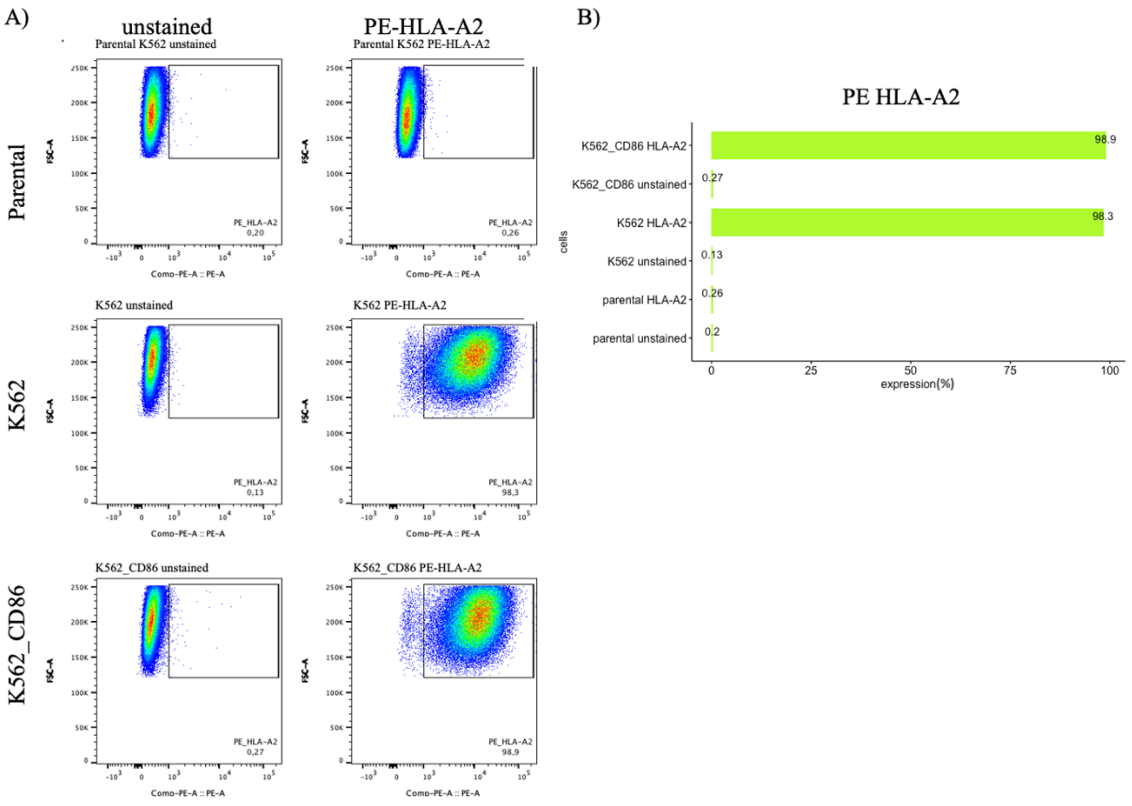

Figure 15. The HLA-A2 expression in K562 based cell lines. (A) Dot plot representation of the HLA-A2 expression. The parental K562 cell line was used as negative control and did not express HLA-A2. The K562 cell line expressed HLA-A2, as well as the K562_CD86 cell line. (B) Bar plot representation of the HLA-A2 expression.

Figure 16 represents the expression of CD86. The aAPC cell line K562_CD86 gets its name from the fact that its CD86 expression has been stabilized, and therefore we expected that only this cell line expresses CD86. The parental K562 cell line's positive cell population was 0.13% in the unstained sample and 0.042% in the stained sample. The corresponding percentages in the K562 cell line was 1.48% and 1.9%, and in the K562_CD86 cell line 0.84% and 91.7%. This indicates that only K562_CD86 has a stabilized CD86 expression and therefore our expectations were met.

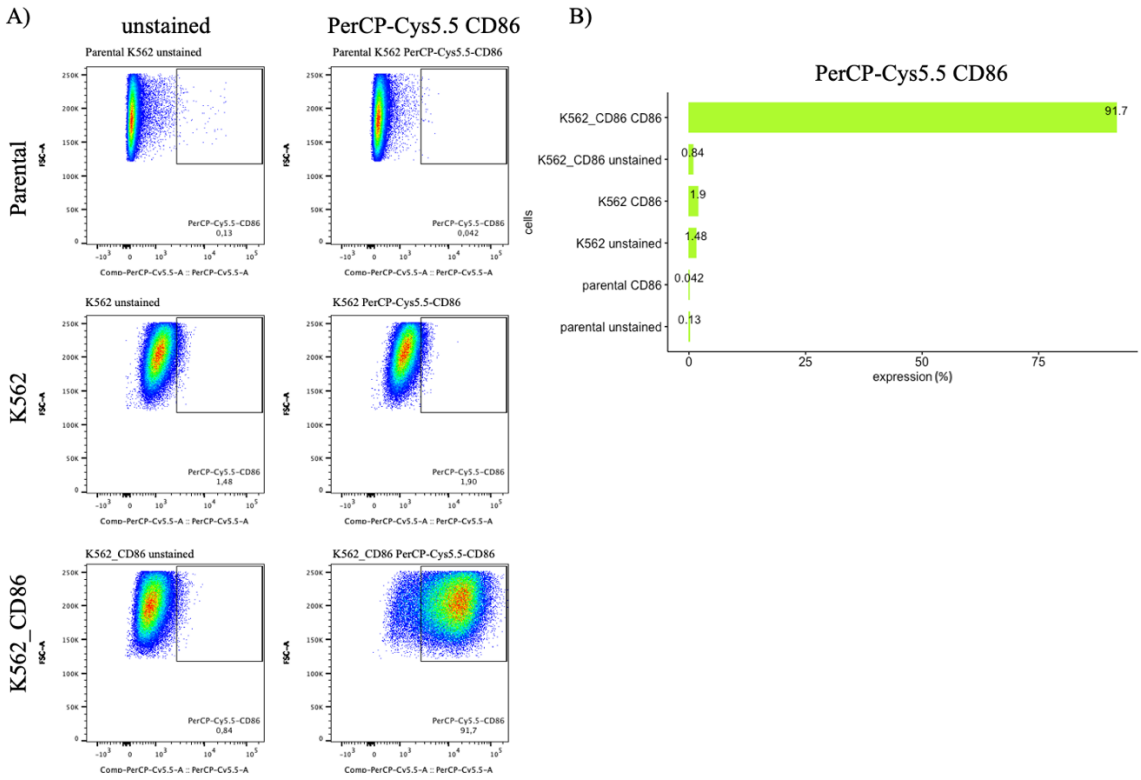

Figure 16. The expression of CD86 in K562 based cell lines. (A) A dot plot representation of the CD86 expression. The parental cell line did not express CD86, nor did the K562 cell line. The K562_CD86 cell line showed a stabilized expression of CD86. (B) Bar plot representation of the CD86 expression.

3.3.6 Activation experiment of the reporter cells

3.3.6.1 Collection of the CFP, GFP and mCherry signals with BD FACSVerse™

We had two reporter cell lines: (i) the triple parameter reporter cell line, Je6.1 TRP, which should display NF-κB-CFP, NFAT-GFP and AP-1-mCherry when activated, and (ii) the single parameter reporter cell line, Je6.1 NFAT, which should display NFAT-GFP when activated. In the activation experiment we stimulated the cells with 1 μM PMA and a with 1 μM, 3 μM, 6 μM and 9 μM ionomycin for 24 hours and then analyzed the protein expression by flow cytometry.

The NFAT-GFP was excited with the blue laser (488 nm) and NF-κB-CFP with the purple laser (405). The BD FACSVerse™ did not have a yellow laser that would be suitable to excite the mCherry fluorochrome, and therefore we did not analyze the AP-1-mCherry parameter.

The NFAT-GFP parameter was analyzed in the FITC channel with the filter 527/32. The NF-κB-CFP was analyzed in the BV421 channel with the filter 448/45. The decision to analyze NF-κB-CFP in the BV421 channel, and not in the more optimal BV510 channel, was made because GFP excitation range overlaps with the BV510 channel and would have given a false positive signal (Figure 17).

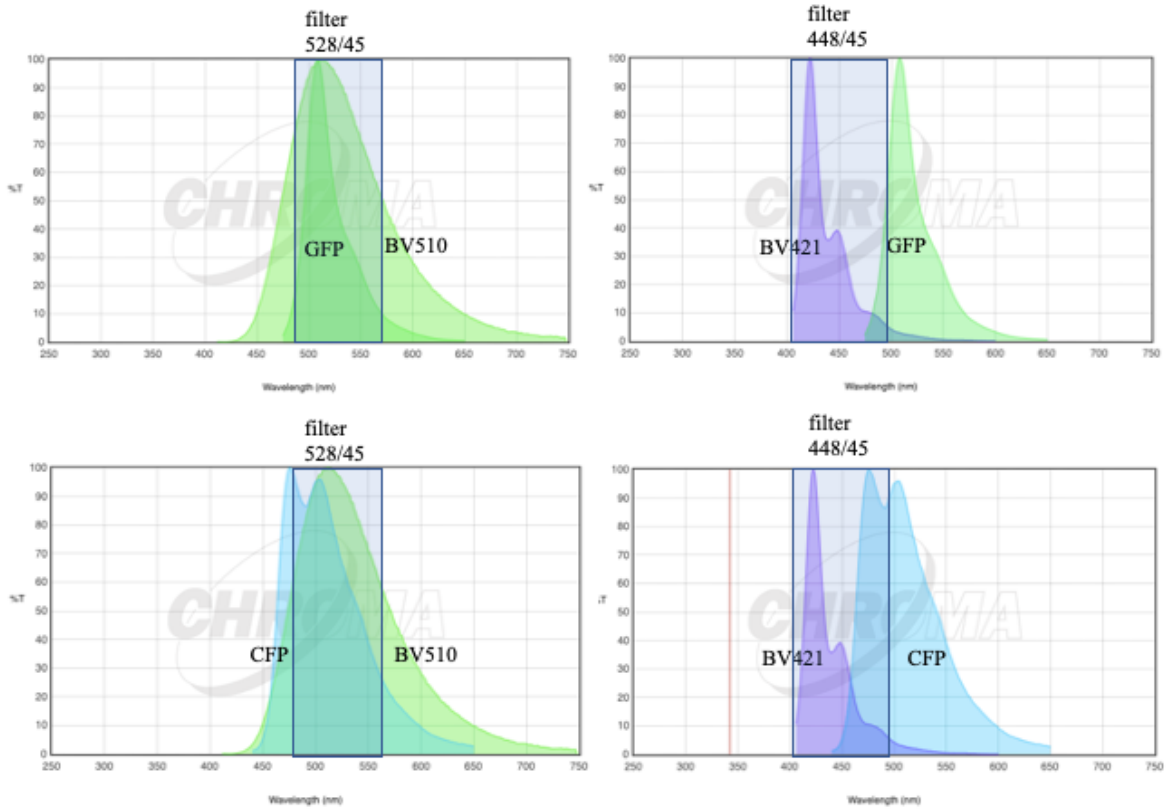

Figure 17. Emission spectra of GFP and CFP and their relation to the channels BV421 and BV510. When analyzing BV510 fluorochrome the flow cytometer collects data with the filter 528/45 and when analyzing BV421 the data is collected with the filter 488/45. The filters are indicated with rectangles and each emission spectra are marked with respective fluorochrome. We can see that GFP overlaps less with the BV421 channel than the BV510 channel (two spectra on the top). We can also see that the CFP overlaps in the same manner (two spectra on the bottom). Our cells express both GFP and CFP. When analyzing CFP expression, the best option is to analyze it in the BV421 channel to minimize signal spill from GFP.

3.3.6.2 Reporter activation using positive control stimulations

In figure 18 the activation results are presented. The Je6.1 NFAT cell line reached maximal protein expression with the lowest concentrations of ionomycine. The Je6.1 TRP cell lines signal got stronger with higher concentration of ionomycine, the NFAT-GFP marker rose

from 13.3 % in the 1 μM ionomycine sample, to 23.7 % in 3 μM ionomycine, and further to 32.1 % in 6 μM ionomycine. At 9 μM ionomycine, the signal descended to 19.8 %.

When comparing the strength of the positive signal between the cell lines, the percentage of cells that reached the strongest signals were 98.3% in Jurkat NFAT NFAT-GFP cell line, 13.3% in the Jurkat TRP NFAT-GFP sample, and 0.08% in the Jurkat TRP NF-κB-CFP sample.

The weakest signal in the Jurkat TRP NF-κB-CFP sample, is due to the different fluorophore CFP, which is weaker than GFP. The difference in signal strength between the Jurkat NFAT and Jurkat TRP cell line, when analyzing the same fluorophore NFAT-GFP, might be a result of the additional modifications of the Jurkat TRP cell line's response elements that facilitates the expression of three fluorescent proteins instead of one. The next step going forwards could be to do a kinetics experiment with 1 μM PMA, where we would take samples at different time stamps to see how quickly the activation signal emerges.

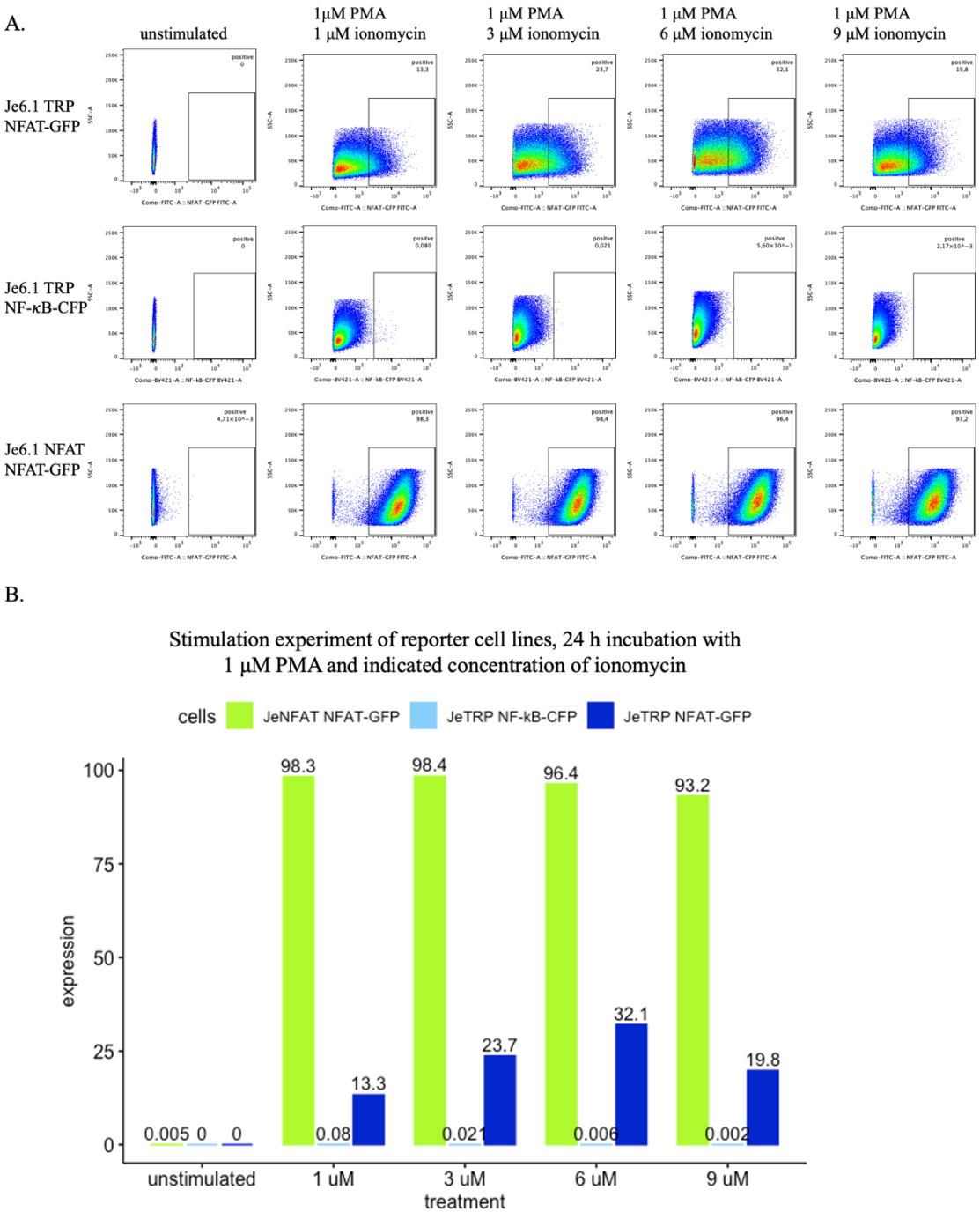

Figure 18. Activation experiment on Je6.1 TRP and Je6.1 NFAT cell lines. (A) The cell lines were stimulated with 1 µM PMA and with the indicated concentration of ionomycin for 24 hours. Following activation, the Jurkat TRP cell line expressed NFAT-GFP and NF-κB-CFP, and the Jurkat NFAT cell line expressed NFAT-GFP. These signals were analyzed with by low cytometry and the results are presented with a dot plot. The Jurkat NFAT cell line

reached maximum activation with the lowest concentration of ionomycine, whereas the Jurkat TRP cell lines got a stronger signal with higher concentrations of ionomycine. (B) A bar plot presenting the difference of the signal strength between the cell lines and fluorophores.

4 Conclusions

The aims of this thesis were to present the biological background of TCR biology, immunotherapies that utilize TCRs, and ways to assess TCR specificity. One of the approaches to assess TCR specificity is reporter cell based co-culture screens. The experimental part's aims were to clone a reconstructed TCR into a vector plasmid, characterize the cell lines used in the co-culture, and optimizing a flow cytometry set up for collecting signals from activated reporter cells. This type of co-culture screen did not exist in the laboratory prior to this project and I have done the groundwork for this screen as a part of my thesis. This work included amplification of TCR chains, assembly of the vector plasmid, sanger sequencing of the inserted TCR chains, characterization of reporter cell lines and aAPC cell lines, as well as activation experiment and signal collection of reporter cells.

Based on the high transformation rate, we conclude that the transformation of the assembled vector to E. coli seems to be working. However, due to the gaps in the sequencing results, we cannot confirm whether the inserts are intact or not. Next step would be to test, if the sequencing result improves with better sample quality, or if there is a problem in the cloning process. When the cloning is validated, we can proceed to producing viral supernatant and transfect the Jurkat reporter cells, since the characterization of the gifted cell lines has shown that the cells are suitable for the screen. The reporter cells do not express an endogenous TCR or the inhibiting protein CD152, and that half of the cell populations express CD8. The more ambiguous results of CD3 and CD28 expression leaves room for more investigation, but do not make the cell unusable for the screen. The reporter cells were activated and expressed the fluorescent markers, and we were able to optimize the collection of the signal with flow cytometry. The K562 cell lines expressed the stabilized HLA-A2 and one of the two cell lines

expressed CD86. In the future we could investigate whether the stabilized costimulatory receptor aids the T-cell activation in the co-culture. When the co-culture is set up, the next step would be to down-scale the set up to 96-well format and to test whether a cognate antigen stimulates specifically A6 TCRs. In the future, this screen would be used in the laboratory to test reconstructed TCRs form clinical patient samples. We could investigate whether tumor-infiltrated T-cells have cancer-specific TCRs and see if these cancer-specific TCRs recognizes or becomes activated by candidate antigens.

Furthermore, with a reporter cell based co-culture screen, it is possible to tune and fix different variables, such as tumor-specific co-stimulatory receptors, and therefore it could be a useful tool to investigate TCR function in a controlled manner (51). Single-cell sequencing gives loads of exact data about TCR sequences that can be sorted with algorithms, but as stated in many articles (48, 49, 54), the lack of functional data of the TCR:pMHC interaction is a bottleneck in reaching the full potential of computational approaches. With co-culture screens it is possible to address the challenge of validating predicted TCR specificity and function in vitro. With more functional data, it could be possible to train algorithms that predict TCR-specificity, neoantingens, and therefore help to develop better TCR-based therapies such as CAR-T cell therapy, TCR-T cell therapy, TIL therapy, and therapeutic cancer vaccines. One can postulate that in the future we are able to do functional predictions of raw TCR data.

Acknowledgements

This work was carried out at the Hematology Research Unit Helsinki. I would like to thank Professor Satu Mustjoki for giving me the opportunity to work in her lab on a very interesting project. I warmly thank Karita Peltonen for guidance during my experiments and valuable comments on the thesis, and for giving me both encouragement and room to grow as a researcher!

I warmly thank all members of HRUH for sharing good times both inside and outside the lab. It has been a privilege to get to know so many great people! Special thanks to Anita, Moon and Jay for the help on scientific problems. Thanks to Dipa, Ella, Sofie, Jani, Jason, Olli, Otso, Helena, Aino, Alma, Amanda and Milla for fun lunch breaks and delicious coffee sessions. I will always remember the summer 2021 as an inspiring time surrounded by warm and dedicated people!

All my friends, family and relatives are thanked for the great time outside the lab. Special thanks to Annika for the thesis writing sessions on Zoom and in Richardsgatans library. Loving thanks to my partner Vilhelm for the great discussions on how to really get to know a field and how to stay excited about it through the challenges. And for being you.

References

1. Murphy K, Travers P, Walport M, Janeway C. Janeway's immunobiology. 8th ed. New York: Garland Science, Taylor & Francis Group, LLC, 2012.

2. Anderson G, Moore NC, Owen JJ, Jenkinson EJ. Cellular interactions in thymocyte development. Annu Rev Immunol. 1996;14:73-99. doi: 10.1146/annurev.immunol.14.1.73. PMID: 8717508.

3. Rudolph MG, Stanfield RL, Wilson IA. How TCRs bind MHCs, peptides, and coreceptors. Annu Rev Immunol. 2006;24:419-66. doi: 10.1146/annurev.immunol.23.021704.115658. PMID: 16551255.

4. Williams A, Peh CA, Elliott T. The cell biology of MHC class I antigen presentation. Tissue Antigens. 2002 Jan;59(1):3-17. doi: 10.1034/j.1399-0039.2002.590103.x. PMID: 11972873.

5. Zamoyska R. CD4 and CD8: modulators of T-cell receptor recognition of antigen and of immune responses? Curr Opin Immunol. 1998 Feb;10(1):82-7. doi: 10.1016/s0952-7915(98)80036-8. PMID: 9523116.

6. Acuto O, Michel F. CD28-mediated co-stimulation: a quantitative support for TCR signalling. Nat Rev Immunol. 2003 Dec;3(12):939-51. doi: 10.1038/nri1248. PMID: 14647476.

7. Macián F, López-Rodríguez C, Rao A. Partners in transcription: NFAT and AP-1. Oncogene. 2001 Apr 30;20(19):2476-89. doi: 10.1038/sj.onc.1204386. PMID: 11402342.

8. Chen L. Co-inhibitory molecules of the B7-CD28 family in the control of T-cell immunity. Nat Rev Immunol. 2004 May;4(5):336-47. doi: 10.1038/nri1349. PMID: 15122199.

9. Gaffen SL. Signaling domains of the interleukin 2 receptor. Cytokine. 2001 Apr 21;14(2):63-77. doi: 10.1006/cyto.2001.0862. PMID: 11356007.

10. Stinchcombe JC, Griffiths GM. Secretory mechanisms in cell-mediated cytotoxicity. Annu Rev Cell Dev Biol. 2007;23:495-517. doi: 10.1146/annurev.cellbio.23.090506.123521. PMID: 17506701.

11. Davis MM, Bjorkman PJ. T-cell antigen receptor genes and T-cell recognition. Nature. 1988 Aug 4;334(6181):395-402. doi: 10.1038/334395a0. Erratum in: Nature 1988 Oct 20;335(6192):744. PMID: 3043226.

12. Garcia KC, Degano M, Pease LR, Huang M, Peterson PA, Teyton L, Wilson IA. Structural basis of plasticity in T cell receptor recognition of a self peptide-MHC antigen. Science. 1998 Feb 20;279(5354):1166-72. doi: 10.1126/science.279.5354.1166. PMID: 9469799.

13. Mora T, Walczak AM. Quantifying lymphocyte receptor diversity. bioRxiv 046870 (2016).

14. Davis MM, Boyd SD. Recent progress in the analysis of αβT cell and B cell receptor repertoires. Curr Opin Immunol. 2019 Aug;59:109-114. doi: 10.1016/j.coi.2019.05.012. Epub 2019 Jul 18. PMID: 31326777; PMCID: PMC7075470.

15. Alberts A, Lewis J, Raff M, Roberts K, Walter P. Molecular biology of the cell. 6th ed. New York: Garland Science, 2002.

16. Maleki Vareki S. High and low mutational burden tumors versus immunologically hot and cold tumors and response to immune checkpoint inhibitors. J Immunother Cancer. 2018 Dec 27;6(1):157. doi: 10.1186/s40425-018-0479-7. PMID: 30587233; PMCID: PMC6307306.

17. Schadendorf D, Hodi FS, Robert C, Weber JS, Margolin K, Hamid O, Patt D, Chen TT, Berman DM, Wolchok JD. Pooled Analysis of Long-Term Survival Data From Phase II and Phase III Trials of Ipilimumab in Unresectable or Metastatic Melanoma. J Clin Oncol. 2015 Jun 10;33(17):1889-94. doi: 10.1200/JCO.2014.56.2736. Epub 2015 Feb 9. PMID: 25667295; PMCID: PMC5089162.

18. Chen DS, Mellman I. Elements of cancer immunity and the cancer-immune set point. Nature. 2017 Jan 18;541(7637):321-330. doi: 10.1038/nature21349. PMID: 28102259.

19. Mariathasan S, Turley SJ, Nickles D, Castiglioni A, Yuen K, Wang Y, Kadel EE III, Koeppen H, Astarita JL, Cubas R, Jhunjhunwala S, Banchereau R, Yang Y, Guan Y, Chalouni C, Ziai J, Şenbabaoğlu Y, Santoro S, Sheinson D, Hung J, Giltnane JM, Pierce AA, Mesh K, Lianoglou S, Riegler J, Carano RAD, Eriksson P, Höglund M, Somarriba L, Halligan DL, van der Heijden MS, Loriot Y, Rosenberg JE, Fong L, Mellman I, Chen DS, Green M, Derleth C, Fine GD, Hegde PS, Bourgon R, Powles T. TGFβ attenuates tumour response to PD-L1 blockade by contributing to exclusion of T cells. Nature. 2018 Feb 22;554(7693):544-548. doi: 10.1038/nature25501. Epub 2018 Feb 14. PMID: 29443960; PMCID: PMC6028240.

20. Pawelec G. Is There a Positive Side to T Cell Exhaustion? Front Immunol. 2019 Jan 29;10:111. doi: 10.3389/fimmu.2019.00111. PMID: 30761152; PMCID: PMC6362299.

21. Thommen DS, Schumacher TN. T Cell Dysfunction in Cancer. Cancer Cell. 2018 Apr 9;33(4):547-562. doi: 10.1016/j.ccell.2018.03.012. PMID: 29634943; PMCID: PMC7116508.

22. Manfredi F, Cianciotti BC, Potenza A, Tassi E, Noviello M, Biondi A, Ciceri F, Bonini C, Ruggiero E. TCR Redirected T Cells for Cancer Treatment: Achievements, Hurdles, and Goals. Front Immunol. 2020 Sep 3;11:1689. doi: 10.3389/fimmu.2020.01689. PMID: 33013822; PMCID: PMC7494743.

23. Upadhaya S, Yu JX, Shah M, Correa D, Partridge T, Campbell J. The clinical pipeline for cancer cell therapies. Nat Rev Drug Discov. 2021 Jul;20(7):503-504. doi: 10.1038/d41573-021-00100-z. PMID: 34088999.

24. Zhao L, Cao YJ. Engineered T Cell Therapy for Cancer in the Clinic. Front Immunol. 2019 Oct 11;10:2250. doi: 10.3389/fimmu.2019.02250. PMID: 31681259; PMCID: PMC6798078.

25. Lin H, Cheng J, Mu W, Zhou J, Zhu L. Advances in Universal CAR-T Cell Therapy. Front Immunol. 2021 Oct 6;12:744823. doi: 10.3389/fimmu.2021.744823. PMID: 34691052; PMCID: PMC8526896.

26. Van Der Bruggen P, Zhang Y, Chaux P, Stroobant V, Panichelli C, Schultz ES, Chapiro J, Van Den Eynde BJ, Brasseur F, Boon T. Tumor-specific shared antigenic peptides recognized by human T cells. Immunol Rev. 2002 Oct;188:51-64. doi: 10.1034/j.1600-065x.2002.18806.x. PMID: 12445281.

27. Rapoport AP, Stadtmauer EA, Binder-Scholl GK, Goloubeva O, Vogl DT, Lacey SF, Badros AZ, Garfall A, Weiss B, Finklestein J, Kulikovskaya I, Sinha SK, Kronsberg S, Gupta M, Bond S, Melchiori L, Brewer JE, Bennett AD, Gerry AB, Pumphrey NJ, Williams D, Tayton-Martin HK, Ribeiro L, Holdich T, Yanovich S, Hardy N, Yared J, Kerr N, Philip S, Westphal S, Siegel DL, Levine BL, Jakobsen BK, Kalos M, June CH. NY-ESO-1-specific TCR-engineered T cells mediate sustained antigen-specific antitumor effects in myeloma. Nat Med. 2015 Aug;21(8):914-921. doi: 10.1038/nm.3910. Epub 2015 Jul 20. PMID: 26193344; PMCID: PMC4529359.

28. Chapuis AG, Egan DN, Bar M, Schmitt TM, McAfee MS, Paulson KG, Voillet V, Gottardo R, Ragnarsson GB, Bleakley M, Yeung CC, Muhlhauser P, Nguyen HN, Kropp LA, Castelli L, Wagener F, Hunter D, Lindberg M, Cohen K, Seese A, McElrath MJ, Duerkopp N, Gooley TA, Greenberg PD. T cell receptor gene therapy targeting WT1 prevents acute myeloid leukemia relapse post-transplant. Nat Med. 2019 Jul;25(7):1064-1072. doi: 10.1038/s41591-019-0472-9. Epub 2019 Jun 24. PMID: 31235963; PMCID: PMC6982533.

29. Nagarsheth NB, Norberg SM, Sinkoe AL, Adhikary S, Meyer TJ, Lack JB, Warner AC, Schweitzer C, Doran SL, Korrapati S, Stevanović S, Trimble CL, Kanakry JA, Bagheri MH, Ferraro E, Astrow SH, Bot A, Faquin WC, Stroncek D, Gkitsas N, Highfill S, Hinrichs CS. TCR-engineered T cells targeting E7 for patients with metastatic HPV-associated epithelial cancers. Nat Med. 2021 Mar;27(3):419-425. doi: 10.1038/s41591-020-01225-1. Epub 2021 Feb 8. PMID: 33558725.

30. Sun Y, Li F, Sonnemann H, Jackson KR, Talukder AH, Katailiha AS, Lizee G. Evolution of $CD8^+$ T Cell Receptor (TCR) Engineered Therapies for the Treatment of Cancer. Cells. 2021 Sep 10;10(9):2379. doi: 10.3390/cells10092379. PMID: 34572028; PMCID: PMC8469972.

31. Rohaan MW, van den Berg JH, Kvistborg P, Haanen JBAG. Adoptive transfer of tumor-infiltrating lymphocytes in melanoma: a viable treatment option. J Immunother Cancer. 2018 Oct 3;6(1):102. doi: 10.1186/s40425-018-0391-1. PMID: 30285902; PMCID: PMC6171186.

32. Scheper W, Kelderman S, Fanchi LF, Linnemann C, Bendle G, de Rooij MAJ, Hirt C, Mezzadra R, Slagter M, Dijkstra K, Kluin RJC, Snaebjornsson P, Milne K, Nelson BH, Zijlmans H, Kenter G, Voest EE, Haanen JBAG, Schumacher TN. Low and variable tumor reactivity of the intratumoral TCR repertoire in human cancers. Nat Med. 2019 Jan;25(1):89-94. doi: 10.1038/s41591-018-0266-5. Epub 2018 Dec 3. PMID: 30510250.

33. Yost KE, Satpathy AT, Wells DK, Qi Y, Wang C, Kageyama R, McNamara KL, Granja JM, Sarin KY, Brown RA, Gupta RK, Curtis C, Bucktrout SL, Davis MM, Chang ALS, Chang HY. Clonal replacement of tumor-specific T cells following PD-1 blockade. Nat Med. 2019 Aug;25(8):1251-1259. doi: 10.1038/s41591-019-0522-3. Epub 2019 Jul 29. PMID: 31359002; PMCID: PMC6689255.

34. Jiménez-Reinoso A, Nehme-Álvarez D, Domínguez-Alonso C, Álvarez-Vallina L. *Synthetic*TILs: Engineered Tumor-Infiltrating Lymphocytes With Improved Therapeutic Potential. Front Oncol. 2021 Feb 16;10:593848. doi: 10.3389/fonc.2020.593848. PMID: 33680923; PMCID: PMC7928359.

35. Butterfield LH. Cancer vaccines. BMJ. 2015 Apr 22;350:h988. doi: 10.1136/bmj.h988. PMID: 25904595; PMCID: PMC4707521.

36. Morse MA, Gwin WR 3rd, Mitchell DA. Vaccine Therapies for Cancer: Then and Now. Target Oncol. 2021 Mar;16(2):121-152. doi: 10.1007/s11523-020-00788-w. Epub 2021 Jan 29. PMID: 33512679; PMCID: PMC7845582.

37. Melief CJ, van Hall T, Arens R, Ossendorp F, van der Burg SH. Therapeutic cancer vaccines. J Clin Invest. 2015 Sep;125(9):3401-12. doi: 10.1172/JCI80009. Epub 2015 Jul 27. PMID: 26214521; PMCID: PMC4588240.

38. Chang J. MHC multimer: A Molecular Toolbox for Immunologists. Mol Cells. 2021 May 31;44(5):328-334. doi: 10.14348/molcells.2021.0052. PMID: 33972472; PMCID: PMC8175149.

39. Abdelaal HM, Cartwright EK, Skinner PJ. Detection of Antigen-Specific T Cells Using In Situ MHC Tetramer Staining. Int J Mol Sci. 2019 Oct 18;20(20):5165. doi: 10.3390/ijms20205165. PMID: 31635220; PMCID: PMC6834156.

40. Simoni Y, Fehlings M, Newell EW. Multiplex MHC Class I Tetramer Combined with Intranuclear Staining by Mass Cytometry. Methods Mol Biol. 2019;1989:147-158. doi: 10.1007/978-1-4939-9454-0_11. PMID: 31077105.

41. Bentzen AK, Hadrup SR. Evolution of MHC-based technologies used for detection of antigen-responsive T cells. Cancer Immunol Immunother. 2017 May;66(5):657-666. doi: 10.1007/s00262-017-1971-5. Epub 2017 Mar 17. PMID: 28314956; PMCID: PMC5406421.

42. Zhang SQ, Ma KY, Schonnesen AA, Zhang M, He C, Sun E, Williams CM, Jia W, Jiang N. High-throughput determination of the antigen specificities of T cell receptors in single cells. Nat Biotechnol. 2018 Nov 12:10.1038/nbt.4282. doi: 10.1038/nbt.4282. Epub ahead of print. PMID: 30418433; PMCID: PMC6728224.

43. Joglekar AV, Li G. T cell antigen discovery. Nat Methods. 2021 Aug;18(8):873-880. doi: 10.1038/s41592-020-0867-z. Epub 2020 Jul 6. PMID: 32632239.

44. Davis MM, Boyd SD. Recent progress in the analysis of αβT cell and B cell receptor repertoires. Curr Opin Immunol. 2019 Aug;59:109-114. doi: 10.1016/j.coi.2019.05.012. Epub 2019 Jul 18. PMID: 31326777; PMCID: PMC7075470.

45. Dash P, Fiore-Gartland AJ, Hertz T, Wang GC, Sharma S, Souquette A, Crawford JC, Clemens EB, Nguyen THO, Kedzierska K, La Gruta NL, Bradley P, Thomas PG. Quantifiable predictive features define epitope-specific T cell receptor repertoires. Nature. 2017 Jul 6;547(7661):89-93. doi: 10.1038/nature22383. Epub 2017 Jun 21. PMID: 28636592; PMCID: PMC5616171.

46. Glanville J, Huang H, Nau A, Hatton O, Wagar LE, Rubelt F, Ji X, Han A, Krams SM, Pettus C, Haas N, Arlehamn CSL, Sette A, Boyd SD, Scriba TJ, Martinez OM, Davis MM. Identifying specificity groups in the T cell receptor repertoire. Nature. 2017 Jul 6;547(7661):94-98. doi: 10.1038/nature22976. Epub 2017 Jun 21. PMID: 28636589; PMCID: PMC5794212.

47. Jokinen E, Huuhtanen J, Mustjoki S, Heinonen M, Lähdesmäki H. Predicting recognition between T cell receptors and epitopes with TCRGP. PLoS Comput Biol. 2021 Mar 25;17(3):e1008814. doi: 10.1371/journal.pcbi.1008814. PMID: 33764977; PMCID: PMC8023491.

48. Bradley P, Thomas PG. Using T Cell Receptor Repertoires to Understand the Principles of Adaptive Immune Recognition. Annu Rev Immunol. 2019 Apr 26;37:547-570. doi: 10.1146/annurev-immunol-042718-041757. Epub 2019 Jan 30. PMID: 30699000.

49. Müller TR, Schuler C, Hammel M, Köhler A, Jutz S, Leitner J, Schober K, Busch DH, Steinberger P. A T-cell reporter platform for high-throughput and reliable investigation of TCR function and biology. Clin Transl Immunology. 2020 Nov 23;9(11):e1216. doi: 10.1002/cti2.1216. PMID: 33251011; PMCID: PMC7681835.

50. Sibener LV, Fernandes RA, Kolawole EM, Carbone CB, Liu F, McAffee D, Birnbaum ME, Yang X, Su LF, Yu W, Dong S, Gee MH, Jude KM, Davis MM, Groves JT, Goddard WA 3rd, Heath JR, Evavold BD, Vale RD, Garcia KC. Isolation of a Structural Mechanism for Uncoupling T Cell Receptor Signaling from Peptide-MHC Binding. Cell. 2018 Jul 26;174(3):672-687.e27. doi: 10.1016/j.cell.2018.06.017. PMID: 30053426; PMCID: PMC6140336.

51. Hu Z, Anandappa AJ, Sun J, Kim J, Leet DE, Bozym DJ, Chen C, Williams L, Shukla SA, Zhang W, Tabbaa D, Steelman S, Olive O, Livak KJ, Kishi H, Muraguchi A, Guleria I, Stevens J, Lane WJ, Burkhardt UE, Fritsch EF, Neuberg D, Ott PA, Keskin DB, Hacohen N, Wu CJ. A cloning and expression system to probe T-cell receptor specificity and assess functional avidity to neoantigens. Blood. 2018 Nov 1;132(18):1911-1921. doi: 10.1182/blood-2018-04-843763. Epub 2018 Aug 27. PMID: 30150207; PMCID: PMC6213317.

52. Kula T, Dezfulian MH, Wang CI, Abdelfattah NS, Hartman ZC, Wucherpfennig KW, Lyerly HK, Elledge SJ. T-Scan: A Genome-wide Method for the Systematic Discovery of T Cell Epitopes. Cell. 2019 Aug 8;178(4):1016-1028.e13. doi: 10.1016/j.cell.2019.07.009. PMID: 31398327; PMCID: PMC6939866.

53. Paria BC, Levin N, Lowery FJ, Pasetto A, Deniger DC, Parkhurst MR, Yossef R, Kim SP, Florentin M, Ngo LT, Ray S, Krishna S, Robbins PF, Rosenberg SA. Rapid Identification and Evaluation of Neoantigen-reactive T-Cell Receptors From Single Cells. J Immunother. 2021 Jan;44(1):1-8. doi: 10.1097/CJI.0000000000000342. PMID: 33086340; PMCID: PMC7725897.

54. Rosskopf S, Leitner J, Paster W, Morton LT, Hagedoorn RS, Steinberger P, Heemskerk MHM. A Jurkat 76 based triple parameter reporter system to evaluate TCR functions and adoptive T cell strategies. Oncotarget. 2018 Apr 3;9(25):17608-17619. doi: 10.18632/oncotarget.24807. PMID: 29707134; PMCID: PMC5915142.

55. Jutz S, Leitner J, Schmetterer K, Doel-Perez I, Majdic O, Grabmeier-Pfistershammer K, Paster W, Huppa JB, Steinberger P. Assessment of costimulation and coinhibition in a triple parameter T cell reporter line: Simultaneous measurement of NF-κB, NFAT and AP-1. J Immunol Methods. 2016 Mar;430:10-20. doi: 10.1016/j.jim.2016.01.007. Epub 2016 Jan 15. PMID: 26780292.

56. Hausmann S, Biddison WE, Smith KJ, Ding YH, Garboczi DN, Utz U, Wiley DC, Wucherpfennig KW. Peptide recognition by two HLA-A2/Tax11-19-specific T cell clones in relationship to their MHC/peptide/TCR crystal structures. J Immunol. 1999 May 1;162(9):5389-97. PMID: 10228016.